
Large Scale Travelling Ionospheric Disturbances LSTIDs: Sources, propagation characteristics, and detection techniques

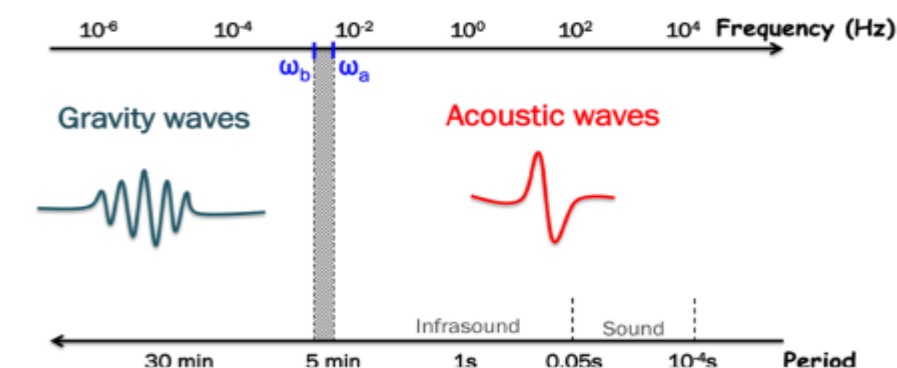
David Altadill

Observatorio del Ebro Fundación (OE), Spain

- **Introduction to TIDs**
 - Large Scale TIDs (LSTID)
 - Medium Scale TIDs (MSTID)
- **Sources of TIDs**
 - External Sources (Coupling from above)
 - Internal Sources (Coupling from below)
- **Propagation characteristics of LSTIDs**
- **Detection techniques of LSTIDs**

Introduction to TIDs

- **Travelling Ionospheric Disturbances (TIDs)**
 - Plasma density fluctuations propagating as waves through the ionosphere at a wide range of velocities and frequencies
 - Ionospheric manifestation of internal atmospheric gravity waves (AGW) in the neutral atmosphere
 - Play an important role in the exchange of momentum and energy between various regions of the upper atmosphere



Waves with $\omega > \omega_a$ are acoustic and propagate through the atmosphere (ω_a acoustic cutoff frequency). Waves with $\omega < \omega_b$ are the gravity waves (ω_b buoyancy or Brunt-Väissälä). Waves with frequencies $\omega_b < \omega < \omega_a$ (shaded rectangle) are evanescent waves and can only propagate horizontally

Hines CO. 1974. The upper atmosphere in motion, Geophysical Monograph, Vol. 18. American Geophysical Union, USA. ISBN: 9780875900186.

Hocke K, Schlegel K. 1996. A review of atmospheric gravity waves and travelling ionospheric disturbances: 1982–1995. Ann Geophys 14: 917–940. <https://doi.org/10.1007/s00585-996-0917-6>.

- **Classification of TIDs (according to wavelength, λ)**
 - Large Scale TIDs (LSTID), $\lambda > 1000$ km.
 - Horizontal velocity $v \approx 400 - 1000$ m s⁻¹ .
 - Temporal Period $T \approx 0.5 - 4$ h .
 - Medium Scale TIDs (MSTID), $\lambda \approx 100 - 600$ km.
 - Horizontal velocity $v \approx 100 - 250$ m s⁻¹ .
 - Temporal Period $T \approx 0.25 - 1$ h .

Hocke K, & Schlegel K. 1996. A review of atmospheric gravity waves and travelling ionospheric disturbances: 1982–1995. Ann Geophys 14: 917–940. <https://doi.org/10.1007/s00585-996-0917-6>.

Fedorenko YP et al. 2013. Model of traveling ionospheric disturbances. J. Space Weather Space Clim., 2013, 3, A30. <https://doi.org/10.1051/swsc/2013052>.

Sources of TIDs

Solar Terminator



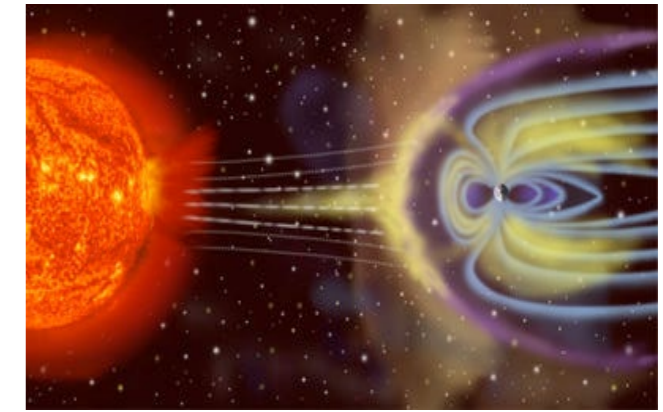
Meteorites



Solar Eclipses



Solar Storms



Impact from external sources – Coupling from above



Impact from internal sources – Coupling from below



Earthquakes



Tsunamis



Volcanoes



Meteorological

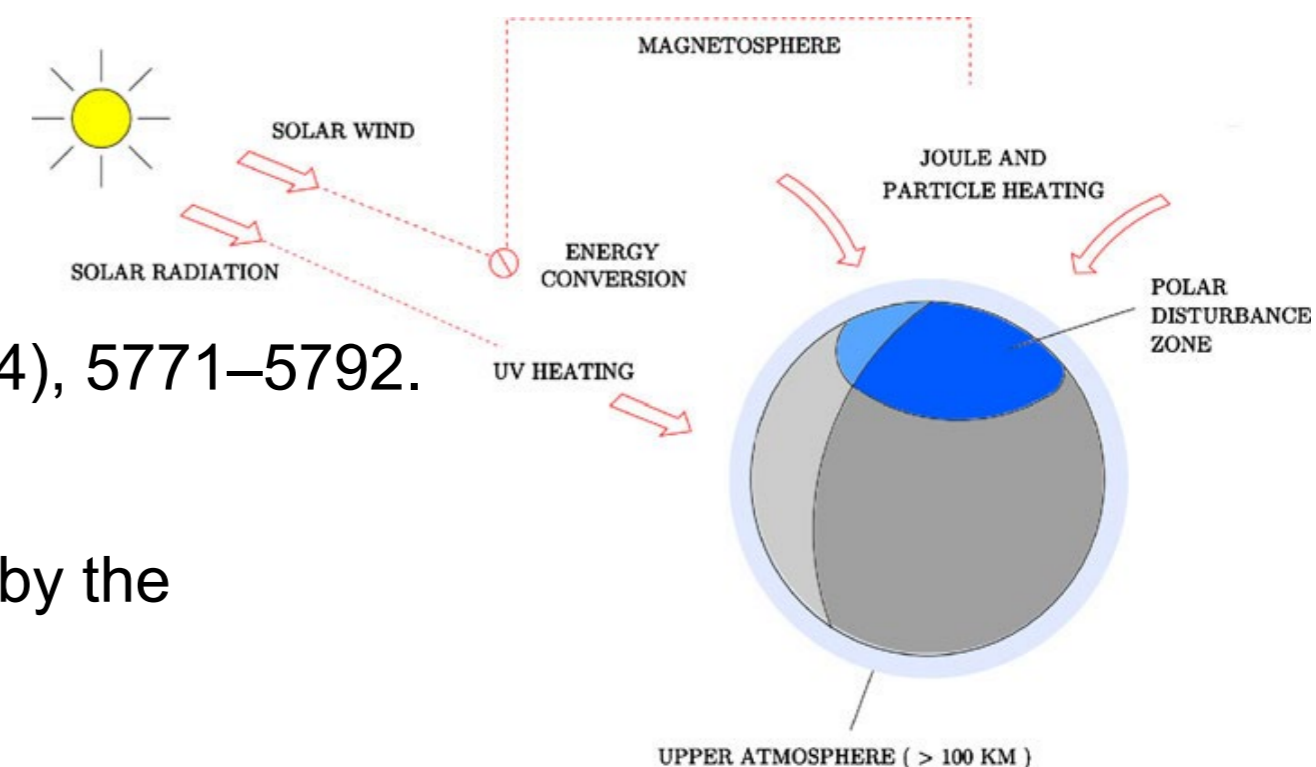
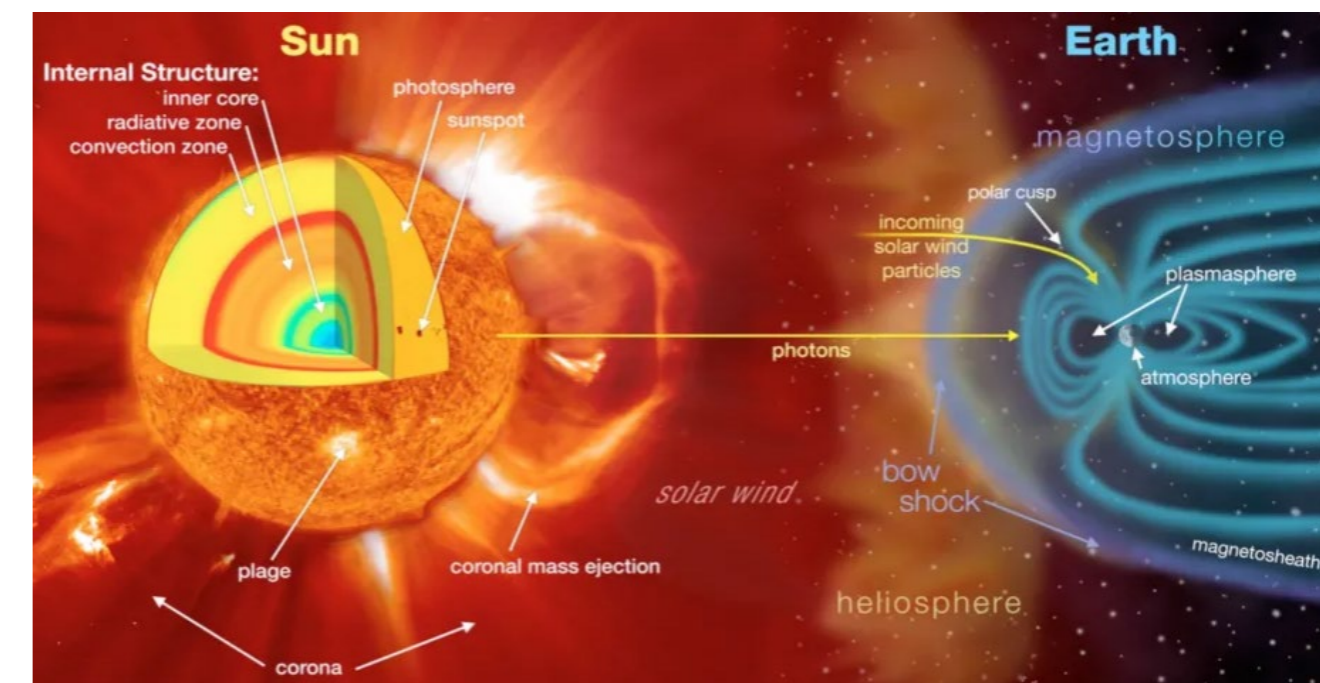


Artificial

- **External (Ionospheric Coupling from above)**

- **Space Weather events.**

- Transitory events originated in the solar activity: Coronal Mass Ejections (**CME**), Corotating Interaction Regions/High Speed Solar wind Streams (**CIR/HSS**), ... carry the particle precipitation in the polar cusp (electrons and protons) and **drive** geomagnetic storms and auroral activity.



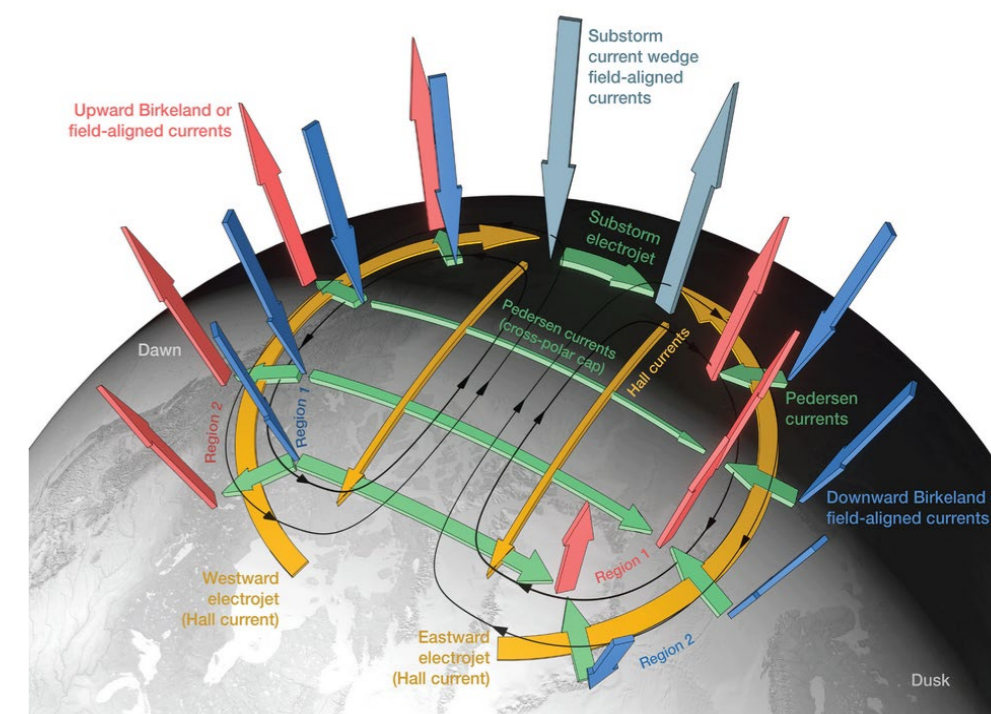
Gonzalez et al. 1994. What is a geomagnetic storm? J Geophys Res 99 (A4), 5771–5792.

<https://doi.org/10.1029/93JA02867>.

Prölss GW. 2011. Density Perturbations in the Upper Atmosphere Caused by the Dissipation of Solar Wind Energy. Surv Geophys 32, 101–195.

<https://doi.org/10.1007/s10712-010-9104-0>.

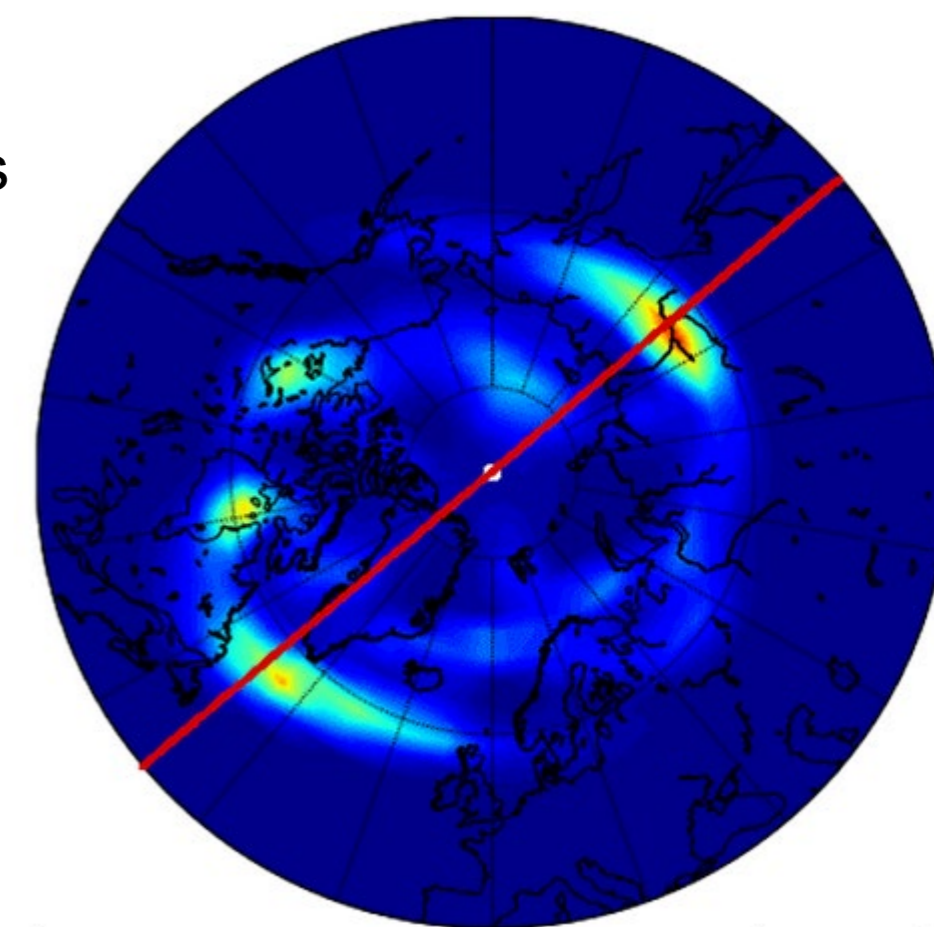
- **External (Ionospheric Coupling from above)**
 - Space Weather events.
 - High latitude thermosphere is heated via the Joule effect during geomagnetically disturbed periods and energy is transferred towards lower latitudes in the form of waves that interact with the ions in the ionospheric plasma.



Palmroth, M et al. 2021. Lower-thermosphere–ionosphere (LTI) quantities: current status of measuring techniques and models, *Ann. Geophys.*, 39, 189–237, <https://doi.org/10.5194/angeo-39-189-2021>.

Prölss GW, Očko M. 2000. Propagation of upper atmospheric storm effects towards lower latitudes. *Adv Space Res* 26: 131–135. [https://doi.org/10.1016/S0273-1177\(99\)01039-X](https://doi.org/10.1016/S0273-1177(99)01039-X).

Paznukhov VV, et al. 2009. Experimental evidence for the role of the neutral wind in the development of ionospheric storms in midlatitudes. *J Geophys Res* 114: A12319. <https://doi.org/10.1029/2009JA014479>.

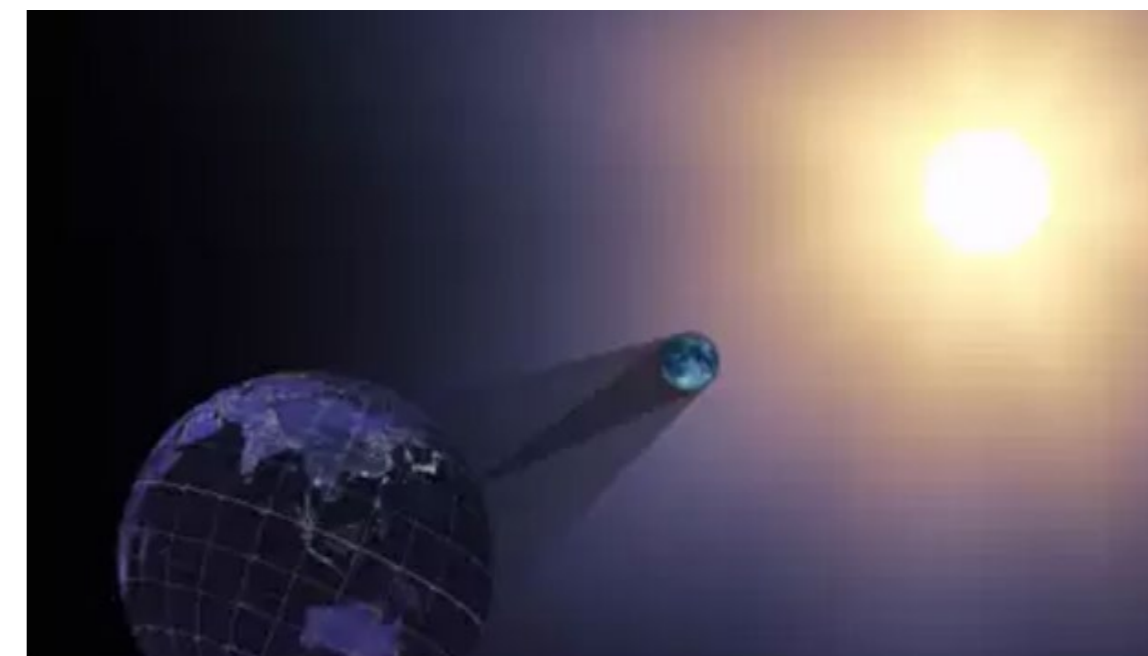


- **External (Ionospheric Coupling from above)**
 - **Solar Eclipses.**
 - Earth's atmosphere and ionosphere are affected by rapid increasing/decreasing ionizing radiation, thermospheric cooling/heating, and changes in the neutral winds, diffusion, and composition.

Chimonas, G, Hines, CO, 1970. Atmospheric gravity waves induced by a solar eclipse. *Journal of Geophysical Research* 75, 875.

<https://doi.org/10.1029/JA075i004p00875>.

Mueller-Wodarg IFC, et al. 1998. Effects of a mid-latitude solar eclipse on the thermosphere and ionosphere: a modelling study. *Geophysical Research Letters* 25, 3787–3790. <https://doi.org/10.1029/1998GL900045>.



This NASA file handout photo illustration shows a visualization animation still image of the Earth, moon, and sun during the eclipse. (Used for representation only)



The Moon casts a shadow on Earth during a total solar eclipse over Europe in this image taken by a French astronaut on the Mir Space Station. Credit: CNES

- **External (Ionospheric Coupling from above)**

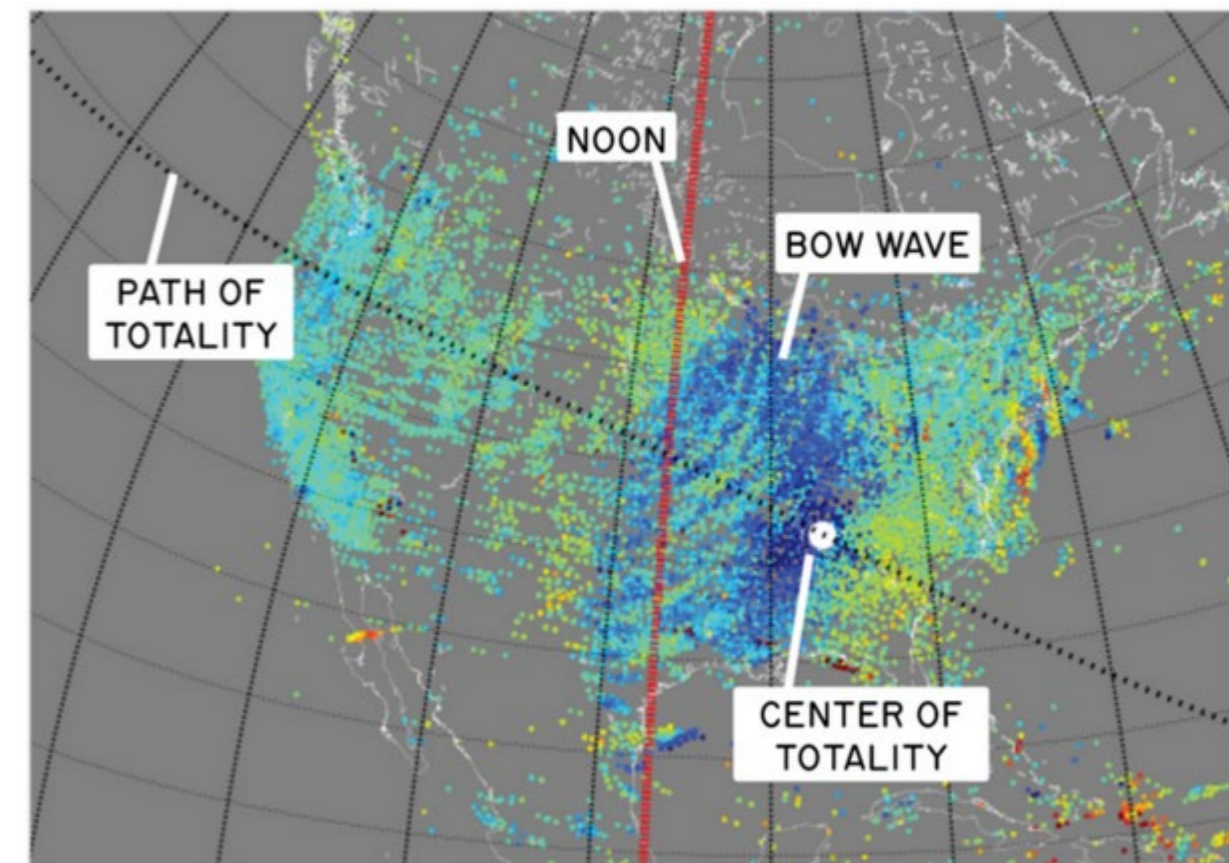
- **Solar Eclipses.**

- The cooling source of Moon's umbra propagating at supersonic speed build up a wave front contributing to generation of AGW.

Altadill D, et al. 2001. Vertical structure of a gravity wave like oscillation in the ionosphere generated by the solar eclipse of August 11, 1999. *Journal of Geophysical Research* 106, 21419–21428.

<https://doi.org/10.1029/2001JA900069>.

Zhang S-R, et al. 2017. Ionospheric bow waves and perturbations induced by the 21 August 2017 solar eclipse. *Geophysical Research Letters*, 44, 12,067–12,073. <https://doi.org/10.1002/2017GL076054>.



- **External (Ionospheric Coupling from above)**
 - **Moving Solar Terminator.**
 - Moving step of atmospheric magnitudes (e.g. pressure, temperature) result in a linear mechanisms for wave excitation of Solar terminator.
 - Atmospheric instabilities inside the Solar Terminator region generate nonlinear mechanisms of wave excitation (e.g., gradient-radiation instability arising from the vertically inhomogeneous absorption of solar radiation, turbulence, and the plasma instability in the evening hours caused by the increase of the electron pressure gradient).

Somsikov VM, 1995. On the mechanism for the formation of atmospheric irregularities in the solar terminator region. *J. Atmos. Terr. Phys.*, 57, 75–83. [https://doi.org/10.1016/0021-9169\(93\)E0017-4](https://doi.org/10.1016/0021-9169(93)E0017-4).

Galushko VG et al., 1998. Incoherent scatter radar observations of AGW/TID events generated by the solar terminator. *Ann. Geophys.*, 16, 821–827. <https://doi.org/10.1007/s00585-998-0821-3>.

- **External (Ionospheric Coupling from above)**

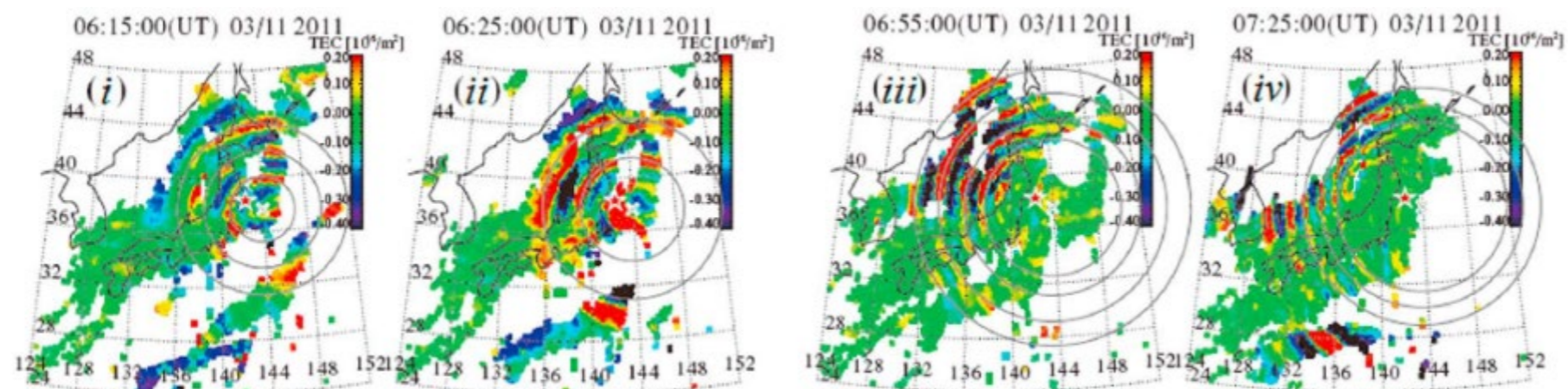
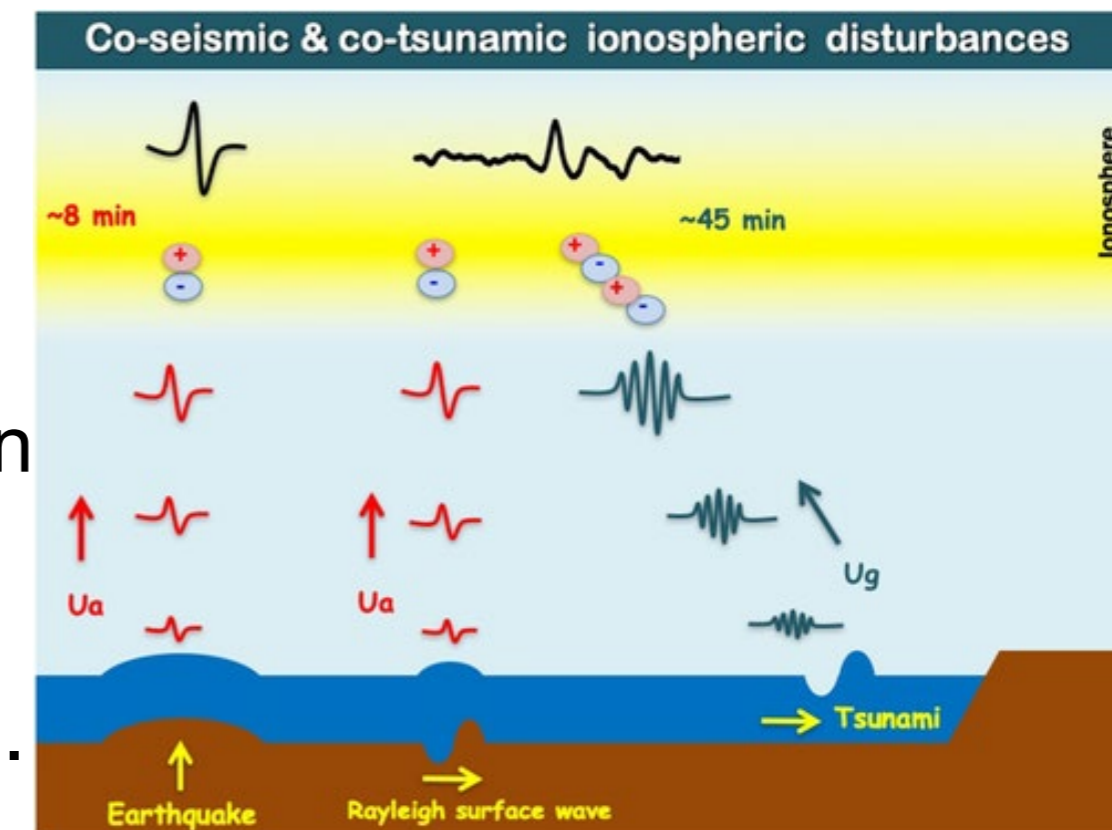
- **Bolides - Meteorites.**

- Acoustic wave driven from the associated burst in the atmosphere launched to the ionosphere and Acoustic Gravity wave driven from the associated burst in the atmosphere again launched to the ionosphere.
- A similar phenomenon to the seismic induced ionospheric disturbances.

Berngardt, OI et al. 2013. Geophysical phenomena accompanying the Chelyabinsk meteoroid impact, Dokl. Earth Sc. 452, 945–947. <https://doi.org/10.1134/S1028334X13090080>.

Perevalova, NP et al. 2015. Ionospheric disturbances in the vicinity of the Chelyabinsk meteoroid explosive disruption as inferred from dense GPS observations, Geophys. Res. Lett., 42, 6535–6543, <https://doi.org/10.1002/2015GL064792>.

- **Internal (Ionospheric Coupling from below)**
 - Earthquake - Tsunamis.
 - Rayleigh wave driven from the associated disturbance in the epicenter are launched to the ionosphere and Acoustic Gravity Wave driven from the associated disturbance epicenter again launched to the ionosphere.



Astafyeva, E. 2019. Ionospheric detection of natural hazards. *Reviews of Geophysics*, 57, 1265–1288.

<https://doi.org/10.1029/2019RG000668>.

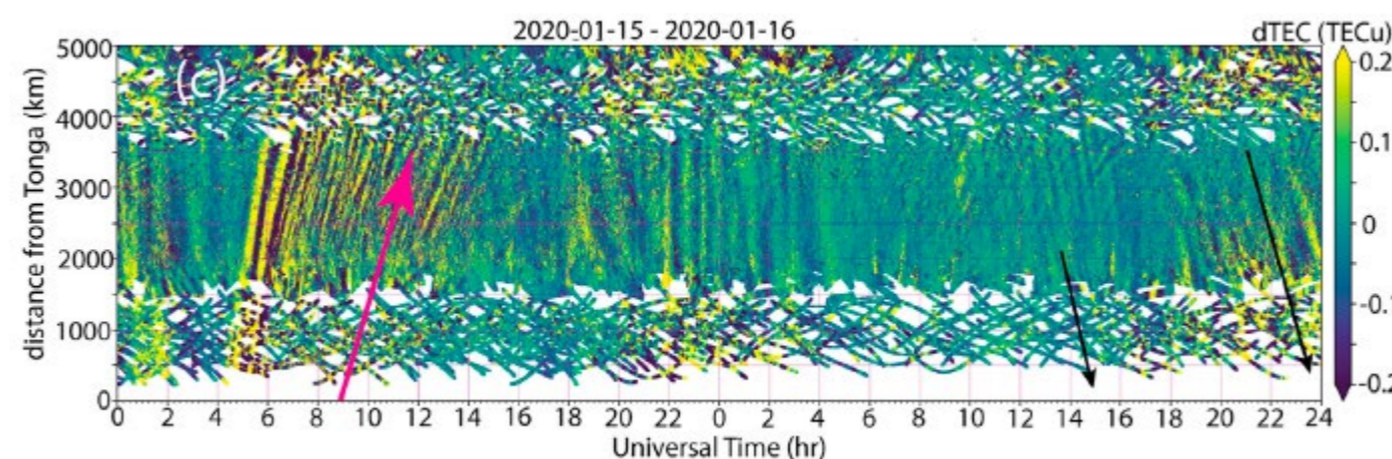
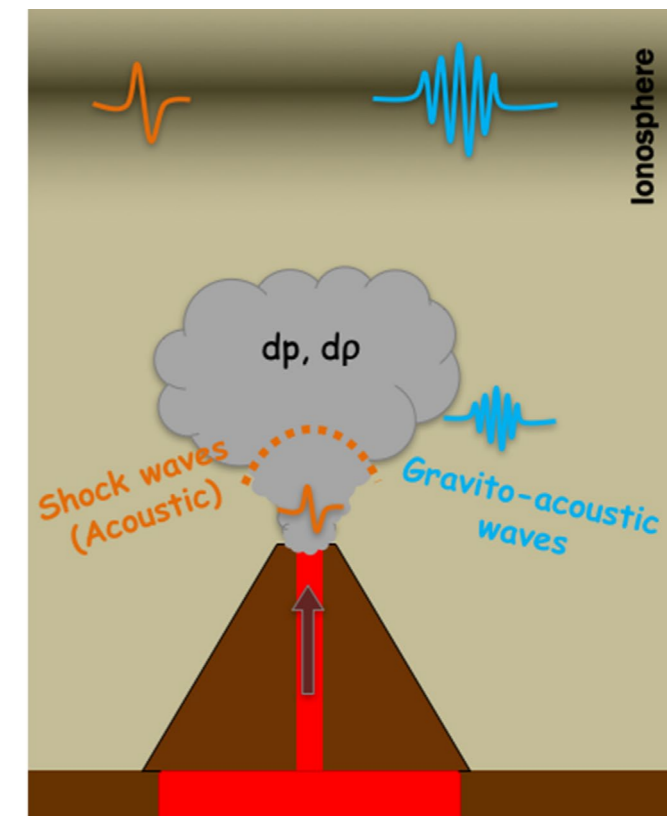
Tsugawa, T et al. 2011. Ionospheric disturbances detected by GPS total electron content observation after the 2011 off the Pacific coast of Tohoku Earthquake, *Earth Planets Space*, 63, 875–879.

<https://doi.org/10.5047/eps.2011.06.035>.

- **Internal (Ionospheric Coupling from below)**

- **Volcanoes.**

- Shock-acoustic waves generated may reach the ionosphere from ~8–9 min after an eruption.
- Sudden changes of local pressure (dp) and density (ρ) may drive AGW reaching the ionosphere by ~45 min the eruption.



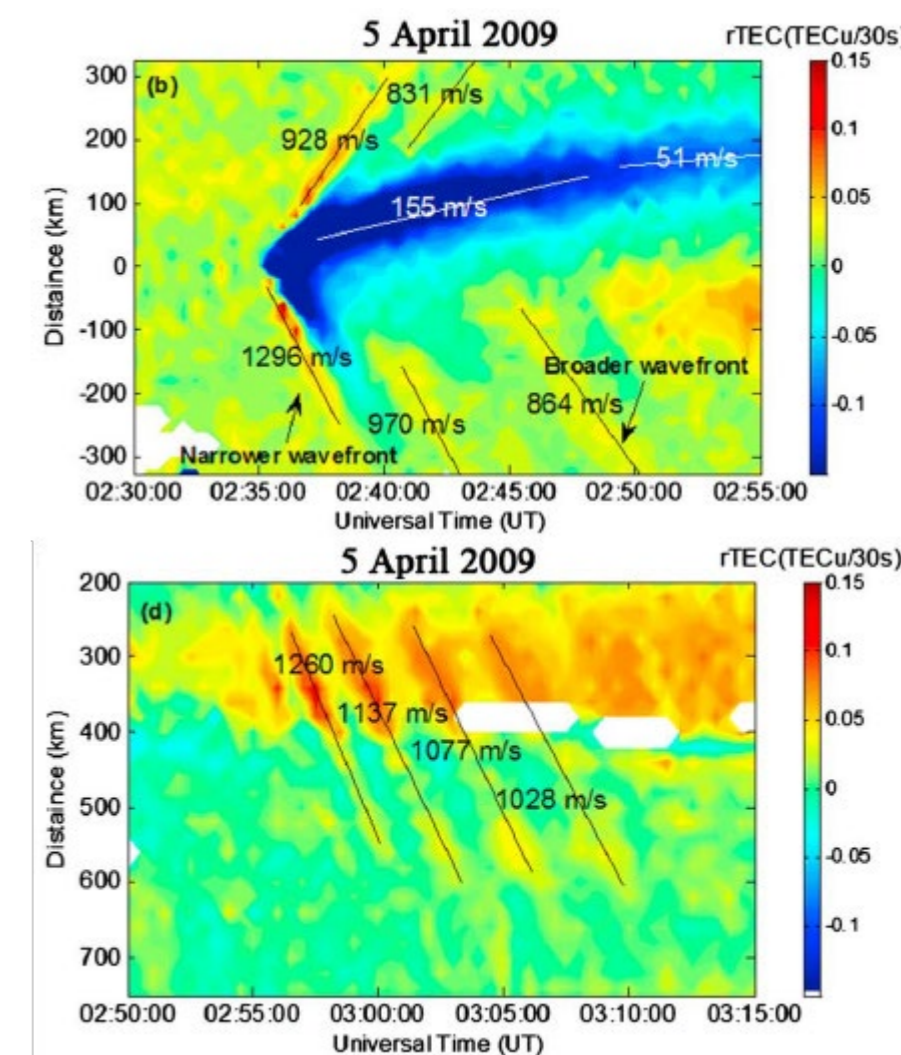
Astafyeva, E. 2019. Ionospheric detection of natural hazards. *Reviews of Geophysics*, 57, 1265–1288. <https://doi.org/10.1029/2019RG000668>.

Zhang S-R et al. 2022. 2022 Tonga Volcanic Eruption Induced Global Propagation of Ionospheric Disturbances via Lamb Waves. *Front. Astron. Space Sci.* 9:871275. <https://doi.org/10.3389/fspas.2022.871275>.

- **Internal (Ionospheric Coupling from below)**

- Rocket launch effects.

- The observed AGW-related TIDs and ionospheric perturbation waves due to the rocket passage are similar to the solar eclipse effect. A localized heat sink traveling through a gravitationally stratified atmosphere with supersonic may result in shock waves observable in the ionospheric plasma perturbation.



Chimonas, G, Hines, CO, 1970. Atmospheric gravity waves induced by a solar eclipse. *Journal of Geophysical Research* 75, 875. <https://doi.org/10.1029/JA075i004p00875>.

Mendillo, M. 1981. The effect of rocket launches on the ionosphere. *Advances in Space Research*, 1(2), 275-290. [https://doi.org/10.1016/0273-1177\(81\)90302-1](https://doi.org/10.1016/0273-1177(81)90302-1).

Lin, CH et al. 201. Observation and simulation of the ionosphere disturbance waves triggered by rocket exhausts, *J. Geophys. Res. Space Physics*, 122, 8868–8882. <https://doi.org/10.1002/2017JA023951>.

- **Internal (Ionospheric Coupling from below)**

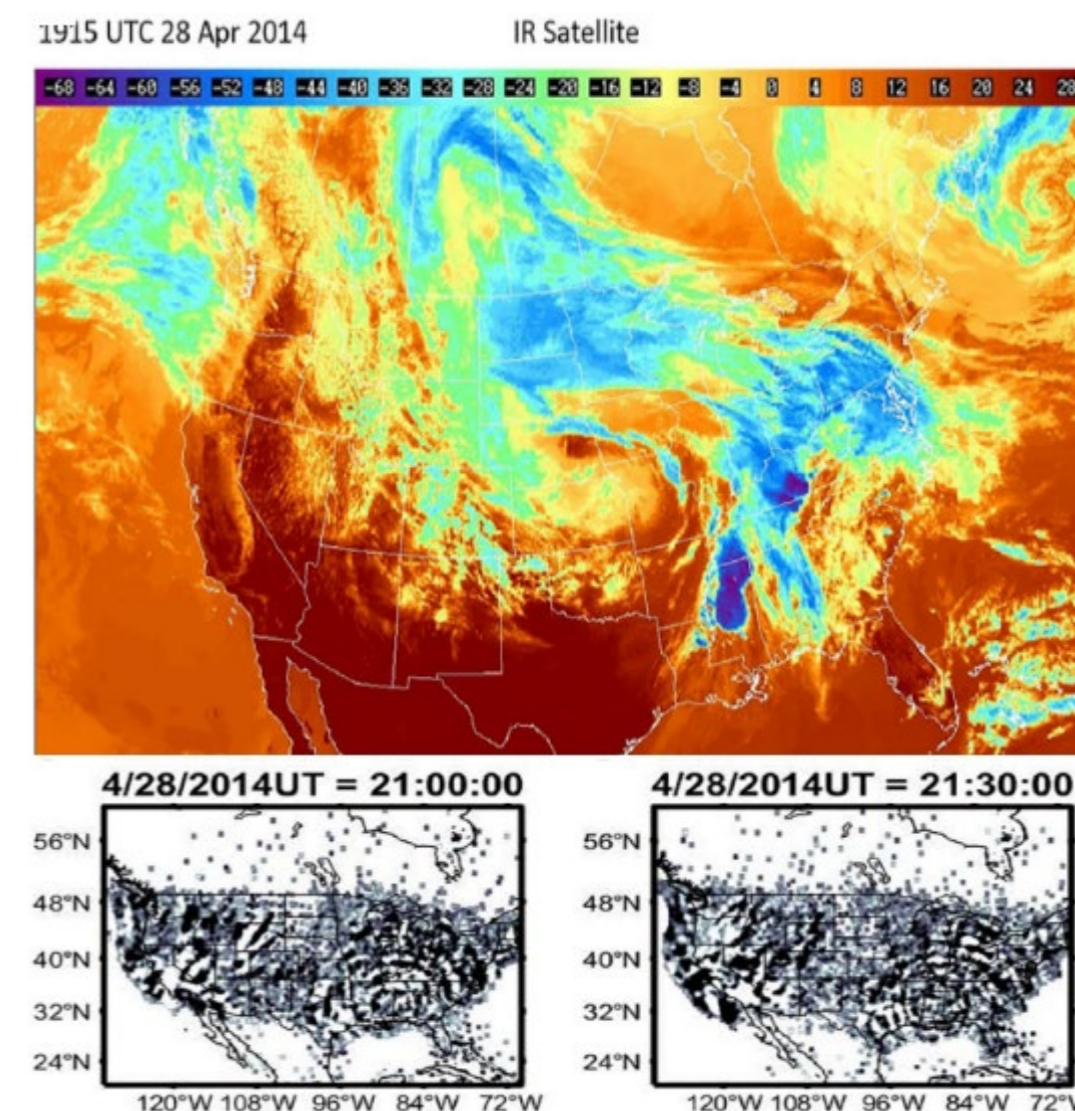
- Meteorological effects.

- Although most primary gravity waves from deep convection break or dissipate in the lower atmosphere, those primary gravity waves with intrinsic phase speeds > 100 m/s can propagate into the thermosphere and ionosphere.

Vadas, S. L. 2007. Horizontal and vertical propagation and dissipation of gravity waves in the thermosphere from lower atmospheric and thermospheric sources, *J. Geophys. Res.*, 112, A06305, <https://doi.org/10.1029/2006JA011845>.

Vadas, S. L., and G. Crowley. 2010. Sources of the traveling ionospheric disturbances observed by the ionospheric TIDDBIT sounder near Wallops Island on 30 October 2007, *J. Geophys. Res.*, 115, A07324, <https://doi.org/10.1029/2009JA015053>.

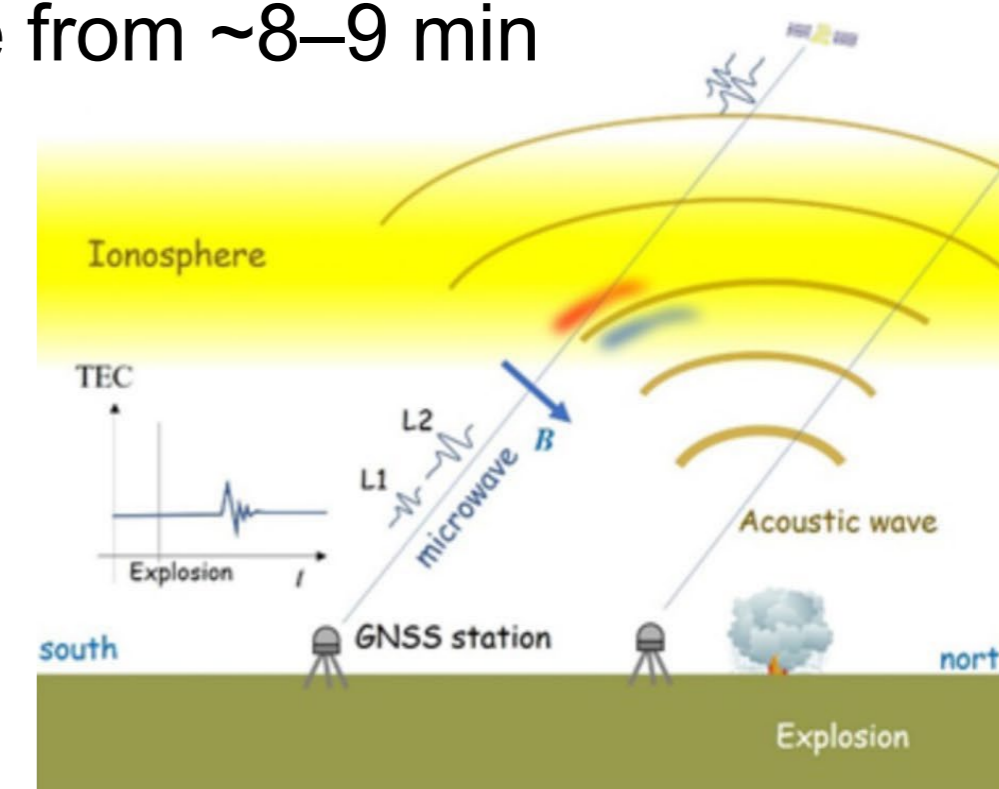
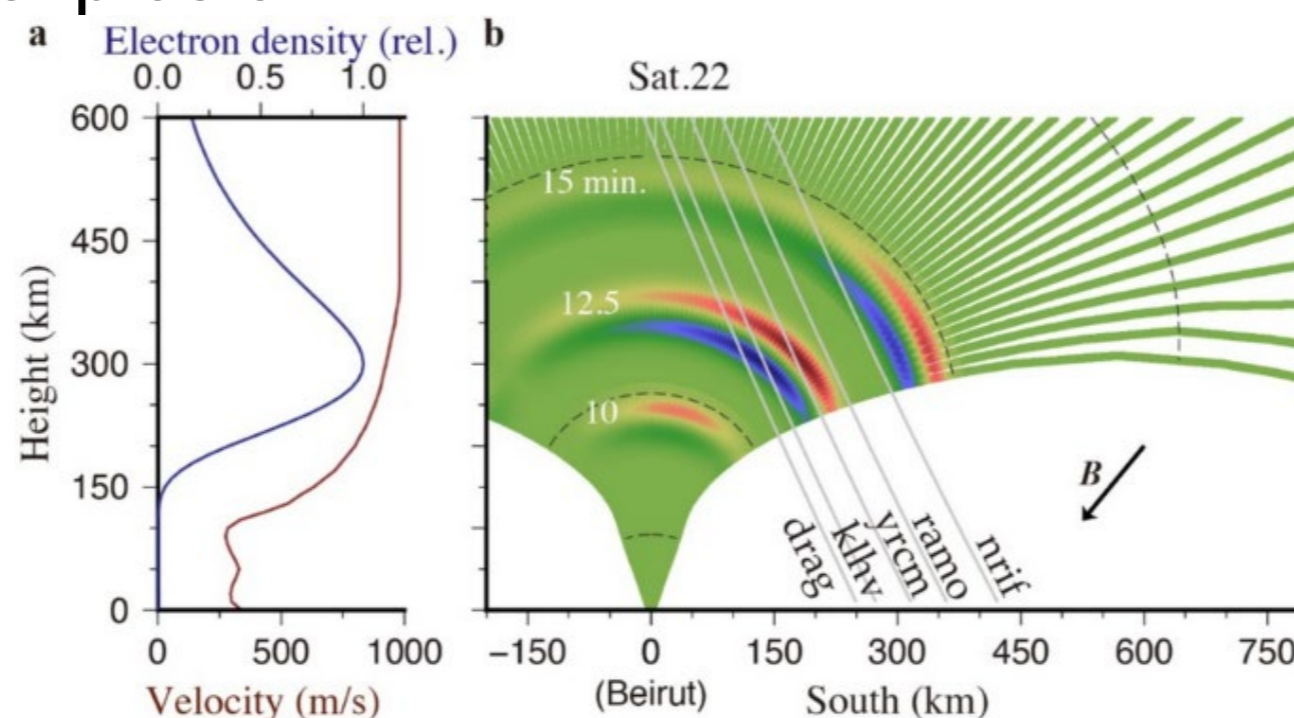
Azeem L. 2007. Spectral Asymmetry of Near-Concentric Traveling Ionospheric Disturbances Due to Doppler-Shifted Atmospheric Gravity Waves, *Front. Astron. Space Sci.* 8:690480, <https://doi.org/10.3389/fspas.2021.690480>.



- **Internal (Ionospheric Coupling from below)**

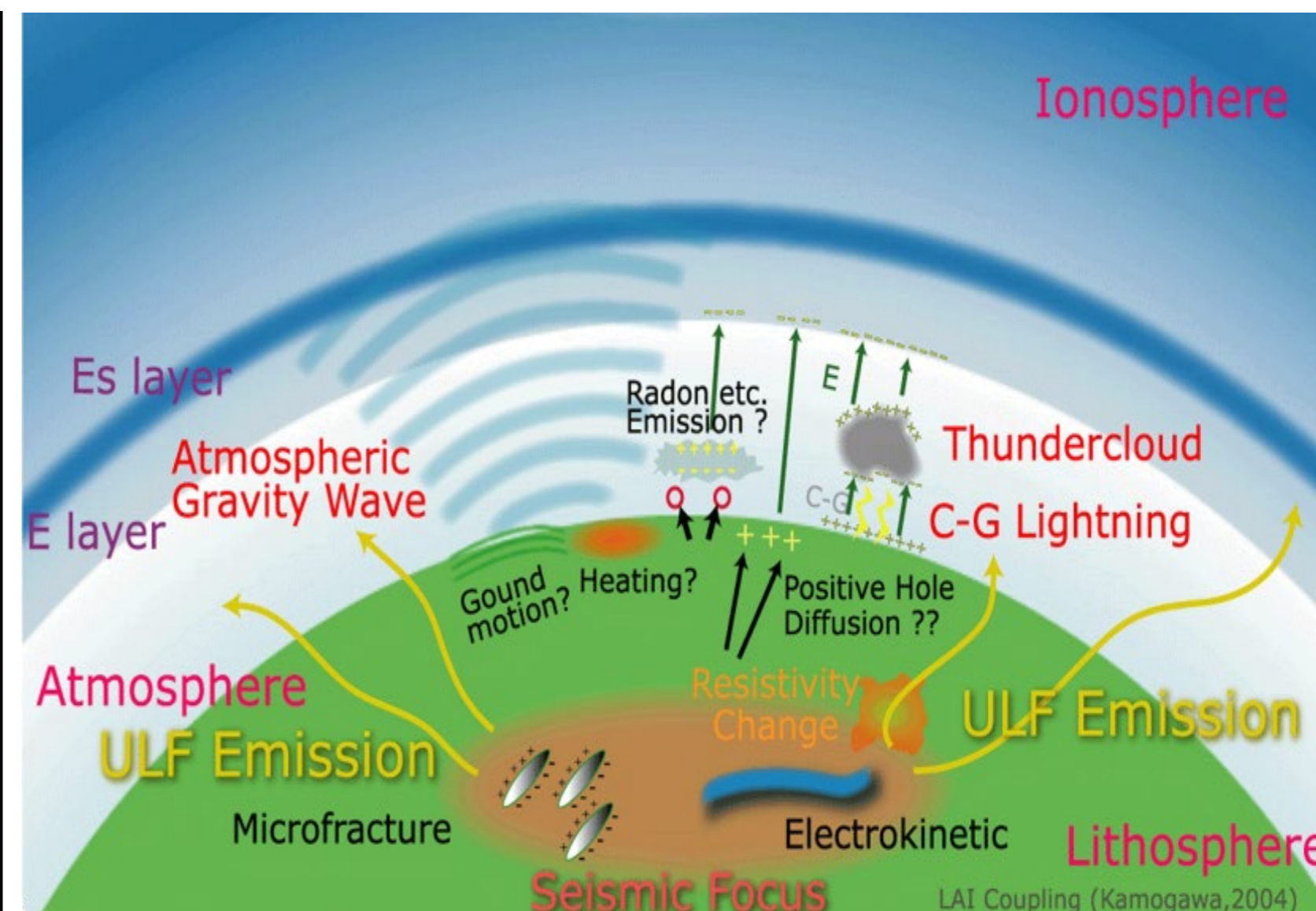
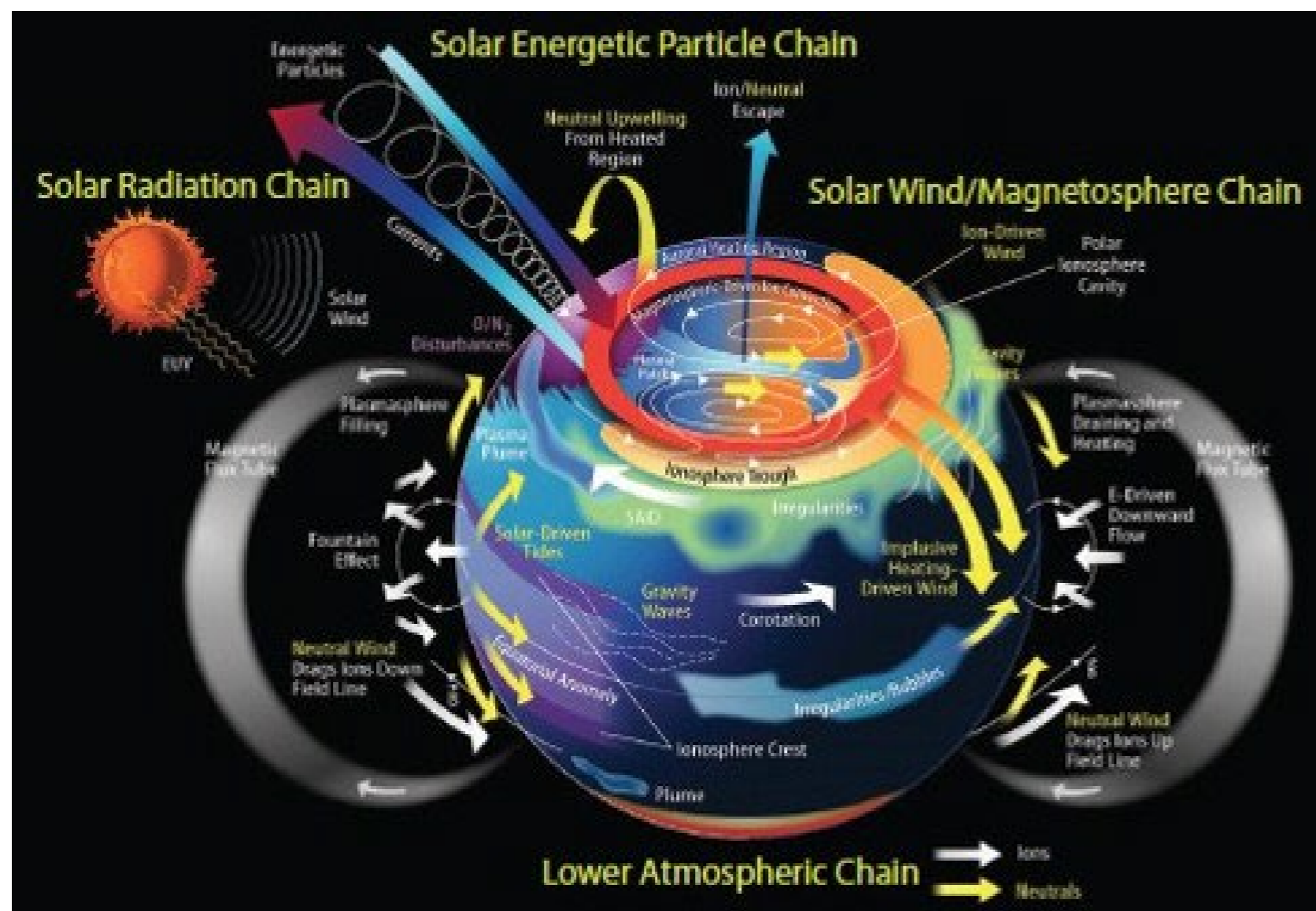
- Artificial explosions.

- Shock-acoustic waves generated may reach the ionosphere from ~8–9 min after a blast or explosion.

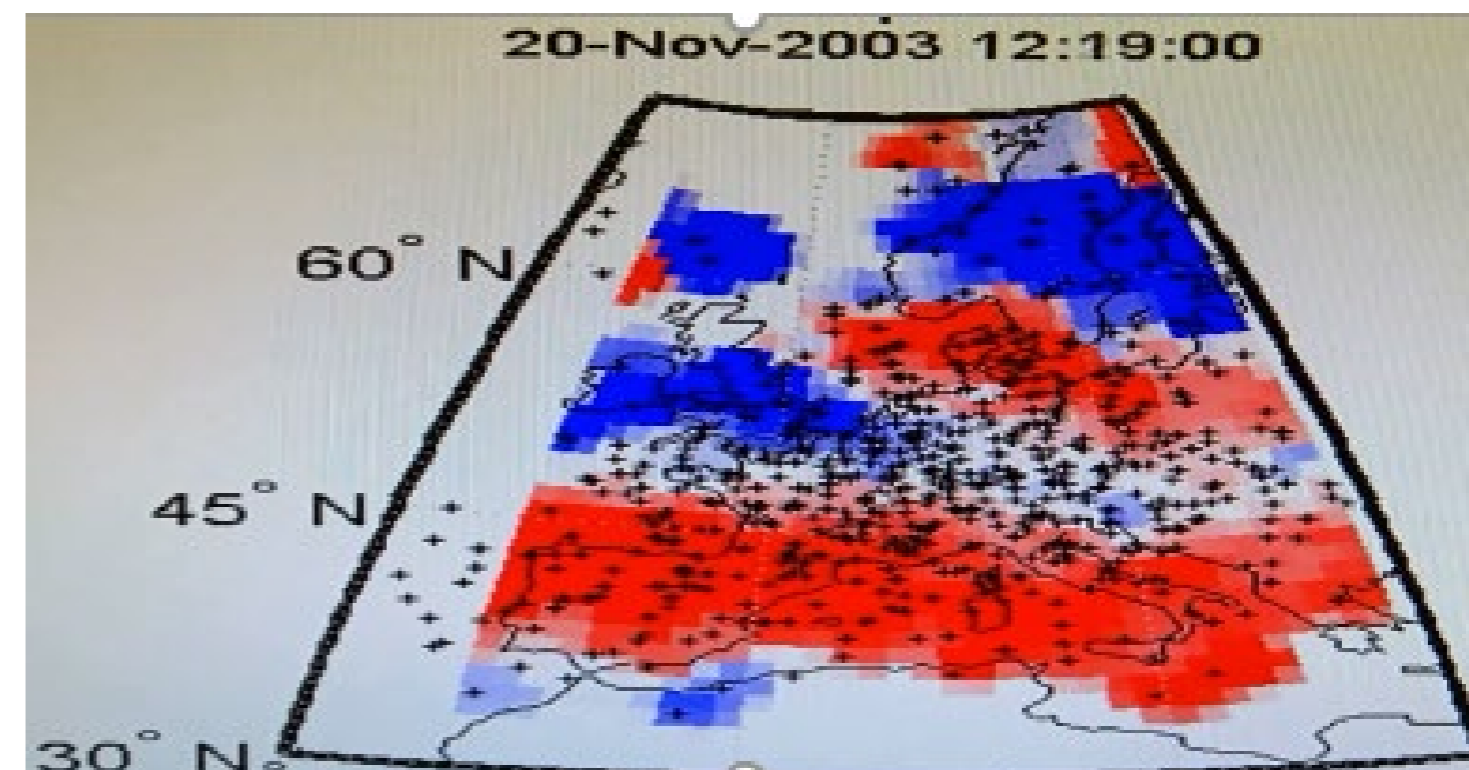
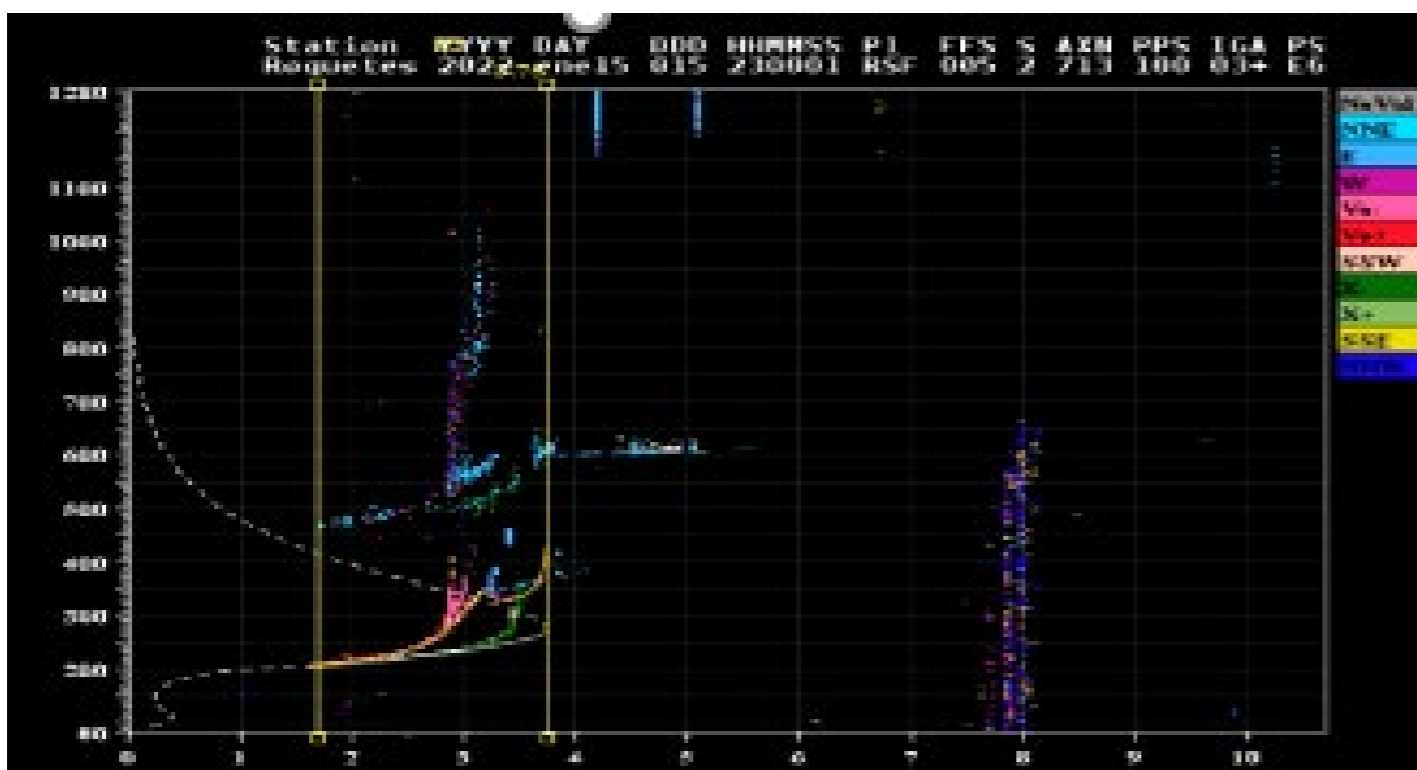


Breitling WJ et al. 1967. Traveling ionospheric disturbances associated with nuclear detonations. *J. Geophys. Res.* 72, 307–315. <https://doi.org/10.1029/JZ072i001p00307>.

Kundu, B et al. 2021. Atmospheric wave energy of the 2020 August 4 explosion in Beirut, Lebanon, from ionospheric disturbances. *Sci Rep* 11, 2793 (2021). <https://doi.org/10.1038/s41598-021-82355-5>.



Sources of TIDs



- **Model perturbation in the background electron density**

- $\Delta N_e(\vec{r}, t) = |\Delta N_e| e^{(i\psi)}$

- \vec{r} - Position, t - time, $|\Delta N_e|$ - Magnitude of the perturbation.

- $\psi = \omega t - \vec{k} \cdot \vec{r} + \tan^{-1} \left[\frac{\sin(I)}{k_{br}} \left(\frac{1}{N_e} \frac{\partial N_e}{\partial z} + k_{zi} \right) \right]$

- \vec{k} - Phase vector, ω - angular frequency, I - Inclination of the magnetic field, k_{br} and k_{zi} - real and imaginary parts of \vec{k} .

- **Assuming no dissipation**

- $k_{zi} = 1/2H$, H - Scale Height, $H = \frac{k_B T}{\bar{\mu} m_u g}$, k_B - Boltzmann's constant, T - Temperature, $\bar{\mu}$ - mean molecular mass, m_u - atomic mass unit, g - acceleration due to gravity.

Hooke, WH. 1968. Ionospheric irregularities produced by internal atmospheric gravity waves, J. Atmos. Terr. Phys., 30, 795–823. [https://doi.org/10.1016/S0021-9169\(68\)80033-9](https://doi.org/10.1016/S0021-9169(68)80033-9).

- **Model perturbation in the background electron density**

- Magnitude electron density perturbation by AGW

$$|\Delta N_e| = N_e U_b(z_0) e^{[k_{zi}(z-z_0)]} \omega^{-1} \sin(I) \cdot \left[\left(\frac{1}{N_e} \frac{\partial N_e}{\partial z} \right) + \left(\frac{k_{br}}{\sin(I)} \right)^2 \right]^{1/2}$$

- N_e - Unperturbed electron density, $U_b(z_0)$ - neutral gas velocity parallel to the magnetic field at reference height z_0 , I - Inclination of the magnetic field, k_{br} and k_{zi} - real and imaginary parts of \vec{k} .
- Valid for below F layer peak.

Hines, CO. 1968. An effect of molecular dissipation in upper atmospheric gravity waves, J. Atmos. Terr. Phys., 30, 845–849. [https://doi.org/10.1016/S0021-9169\(68\)80036-4](https://doi.org/10.1016/S0021-9169(68)80036-4).

- **Model perturbation in the background electron density**

- Assuming planar phase fronts of the AGW & direction of travel is parallel to one of the horizontal axes:

$$\vec{k} = k(k, 0, m), \quad m^2 = k_{zi} \left(\frac{\omega_B^2}{\omega^2} - 1 \right) + \frac{(\omega^2 - \omega_B^2)}{c^2}$$

- ω_B - buoyancy or Brunt-Väissälä frequency, ω_a - acoustic cutoff frequency, c - speed of sound. AGW $\omega < \omega_a$.

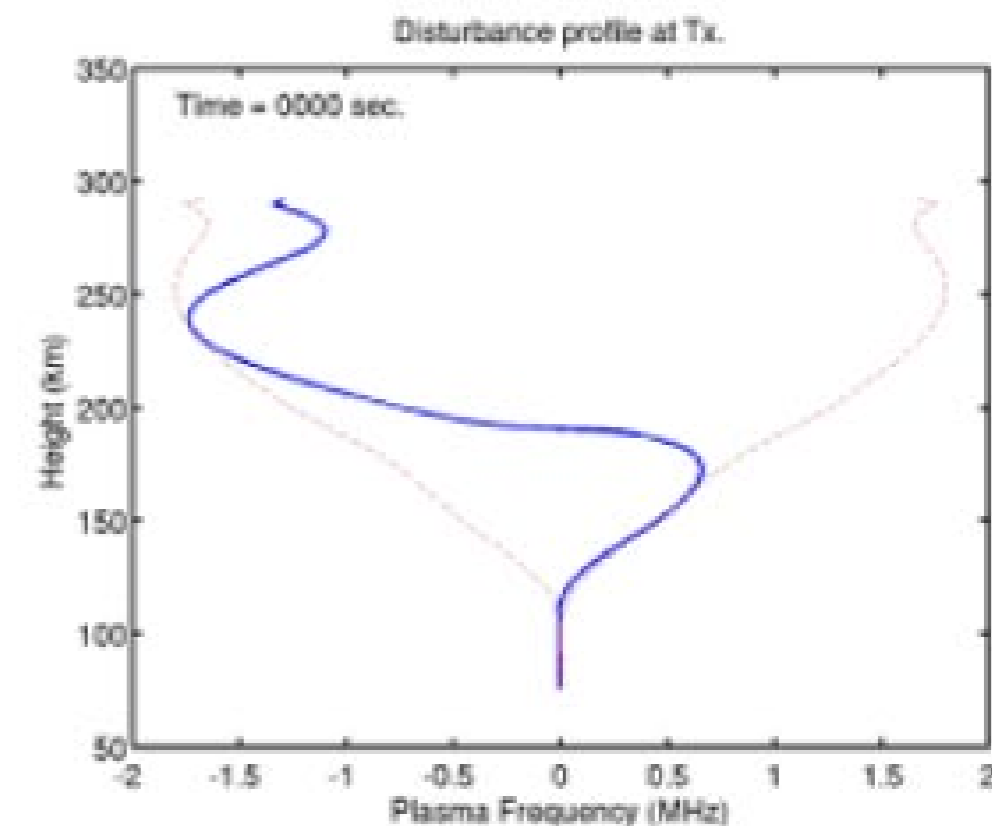
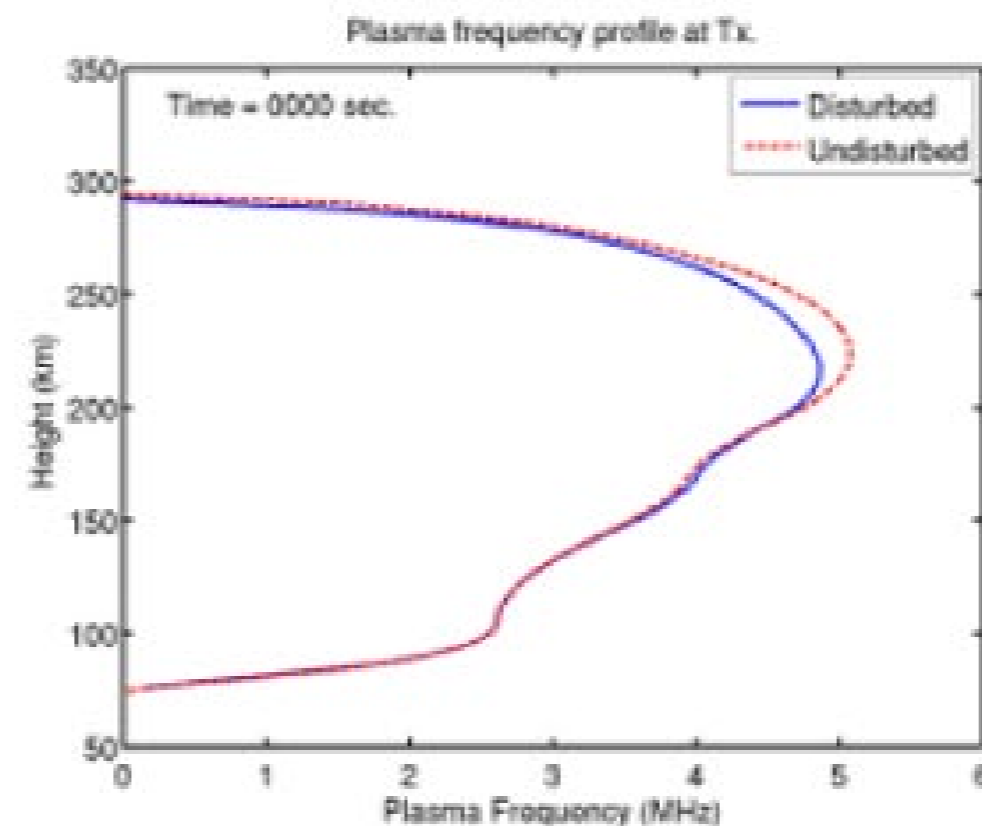
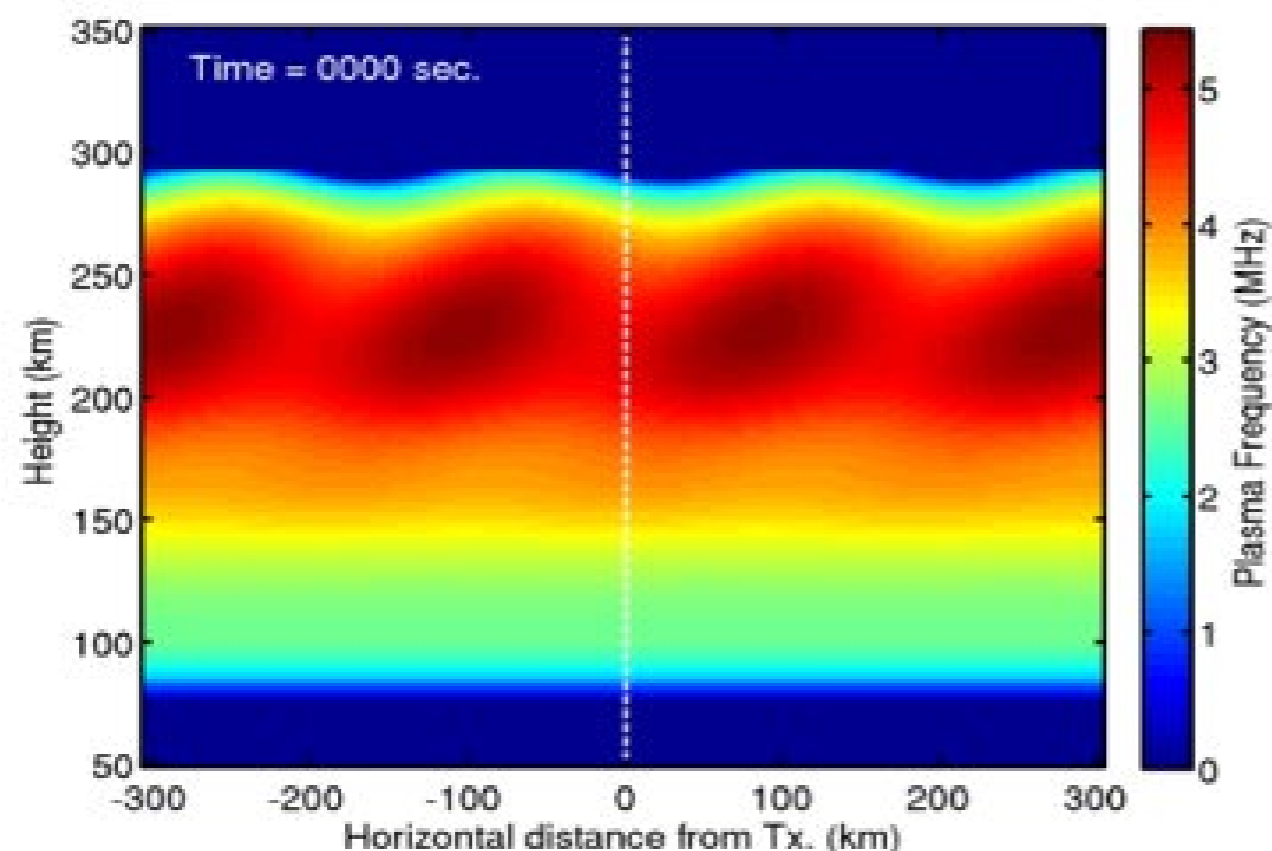
$$\omega_B = \frac{(\gamma-1)g}{\gamma H}, \quad c = \sqrt{\gamma g H}, \quad \omega_a = \frac{c}{2H}$$

- γ - ratio of the specific heat of dry air at constant pressure to the specific heat at constant volume, c - speed of sound.

Cervera, MA and TJ Harris. 2014. Modeling ionospheric disturbance features in quasi-vertically incident ionograms using 3-D magnetoionic ray tracing and atmospheric gravity waves, J. Geophys. Res. Space Physics, 119, 431–440,, <https://doi.org/10.1002/2013JA019247>.

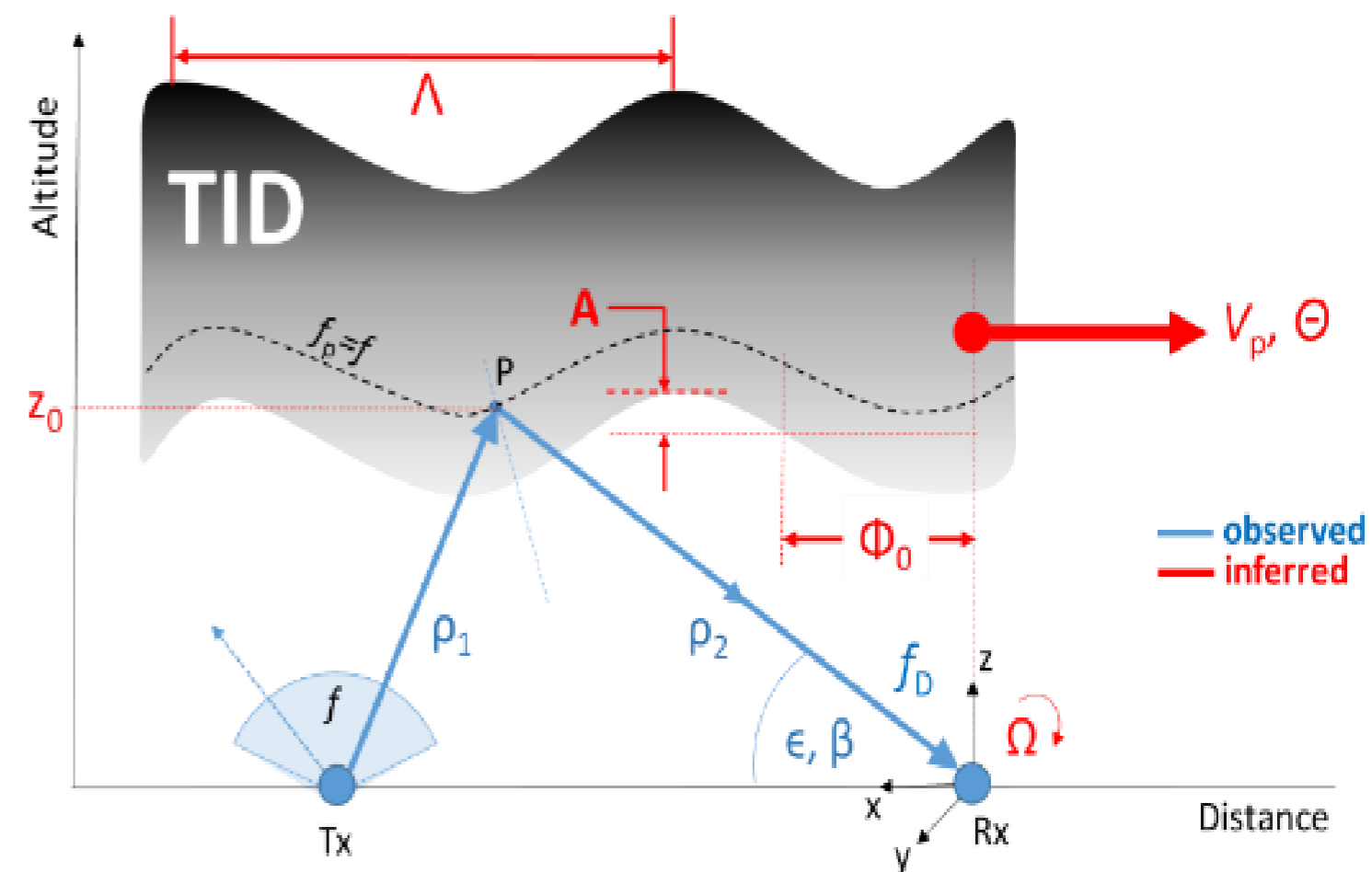
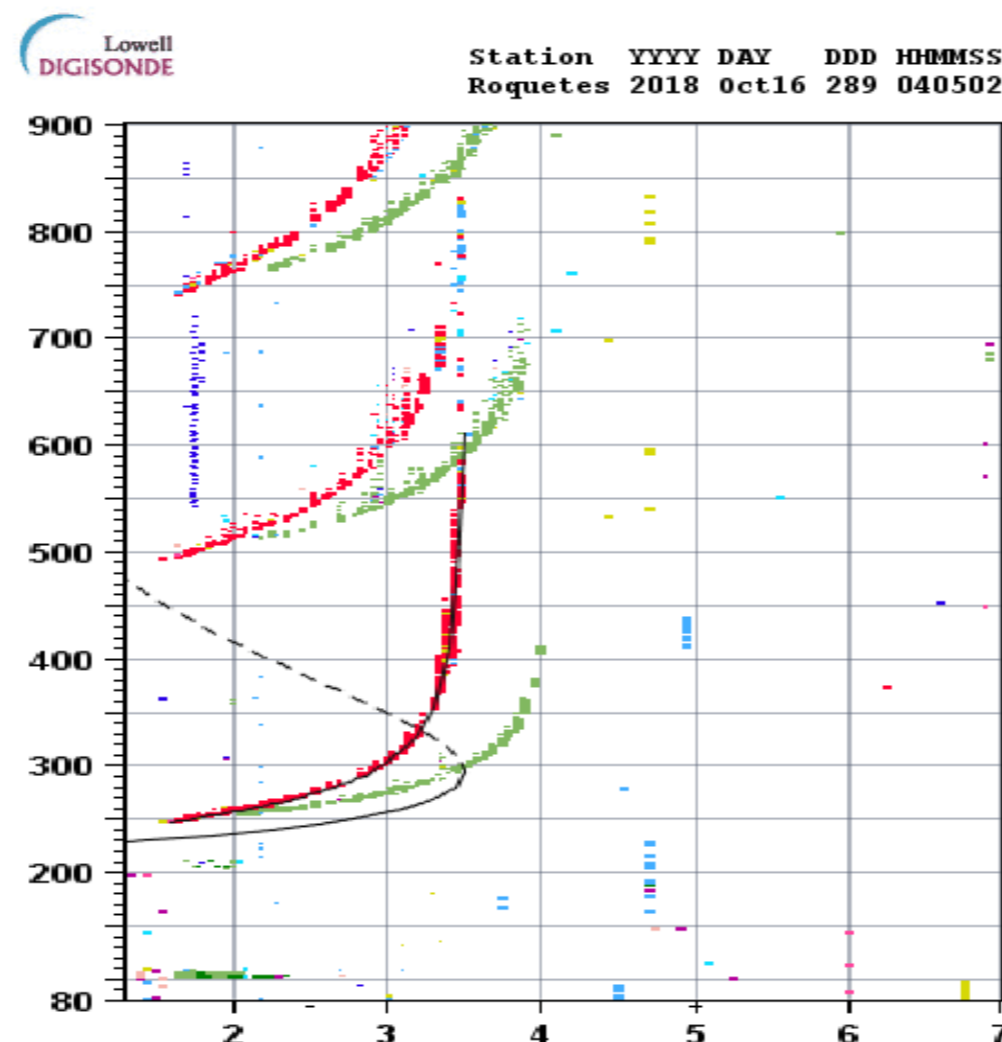
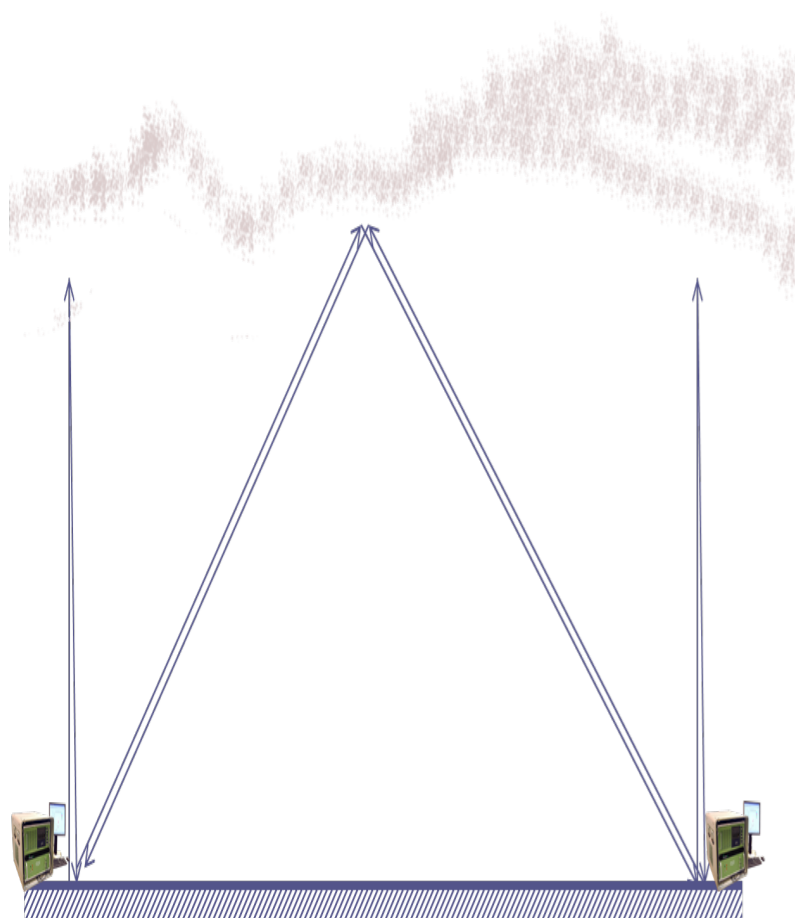
- **Model perturbation in the background electron density**

- TID generated by AGW in Australian region, traveling in the direction 225° from N. With $\lambda = 200$ km, $T = 20$ min, and $U_b = 15$ ms^{-1} , $z_0 = 250$ km. TID tilted by 55° ,



Cervera, MA and TJ Harris. 2014. Modeling ionospheric disturbance features in quasi-vertically incident ionograms using 3-D magnetoionic ray tracing and atmospheric gravity waves, *J. Geophys. Res. Space Physics*, 119, 431–440,, <https://doi.org/10.1002/2013JA019247>.

- Ground Based sensors

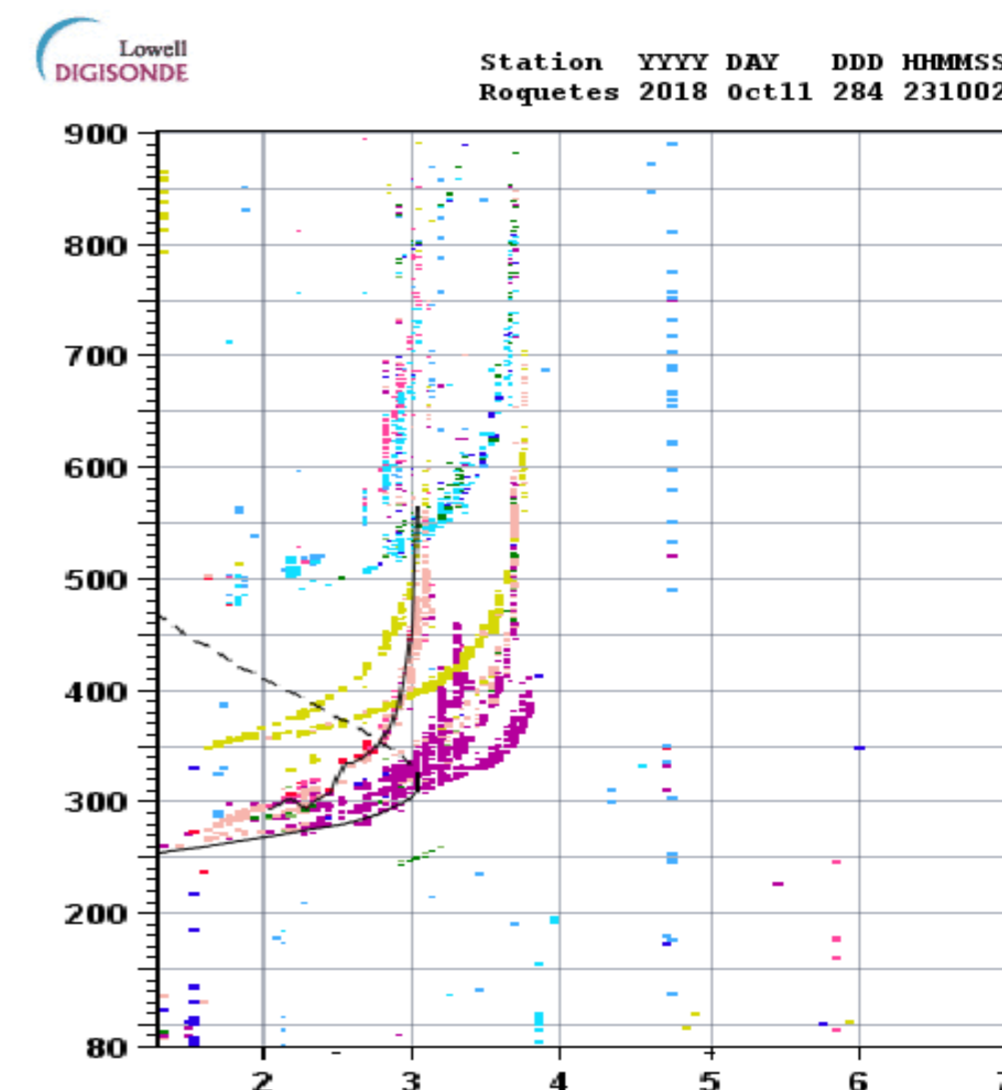
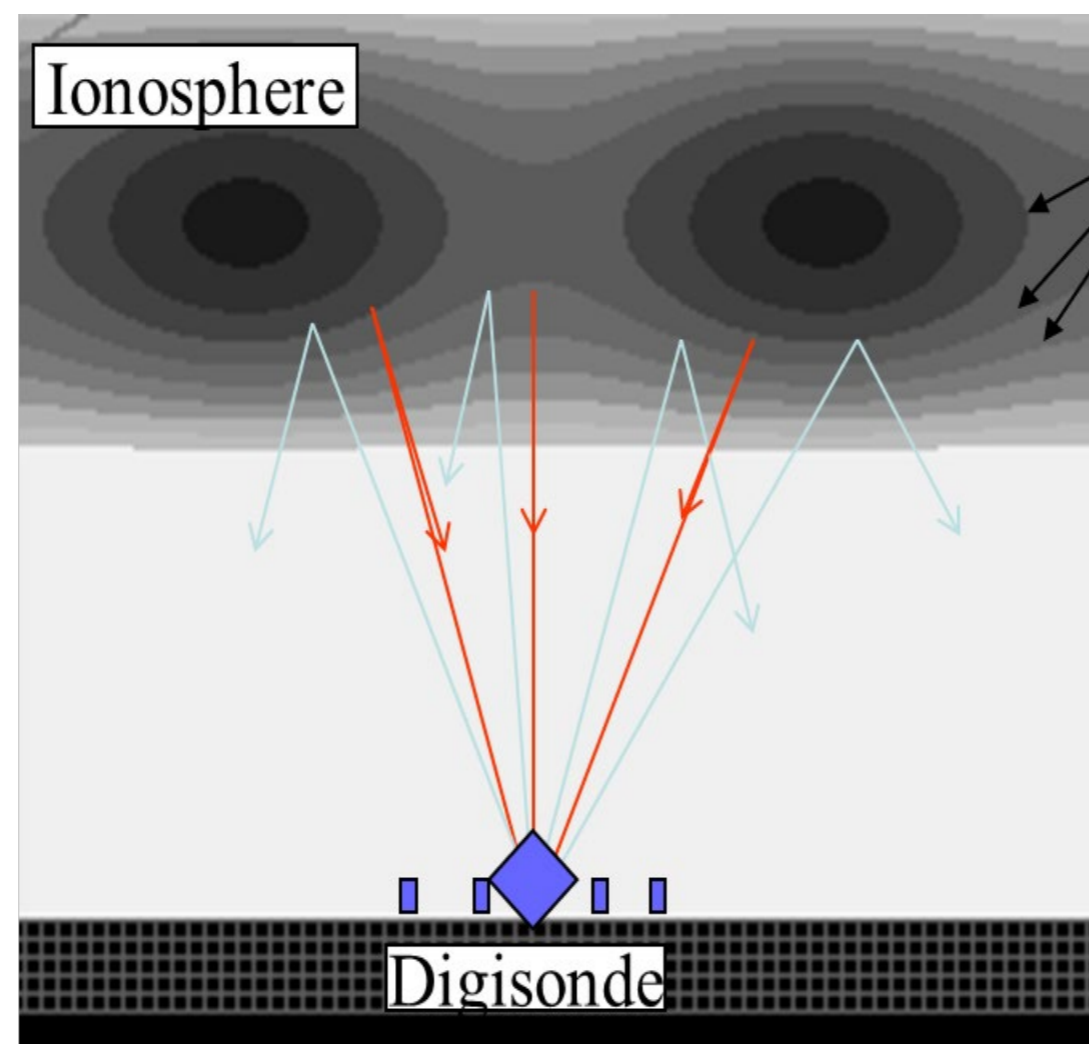
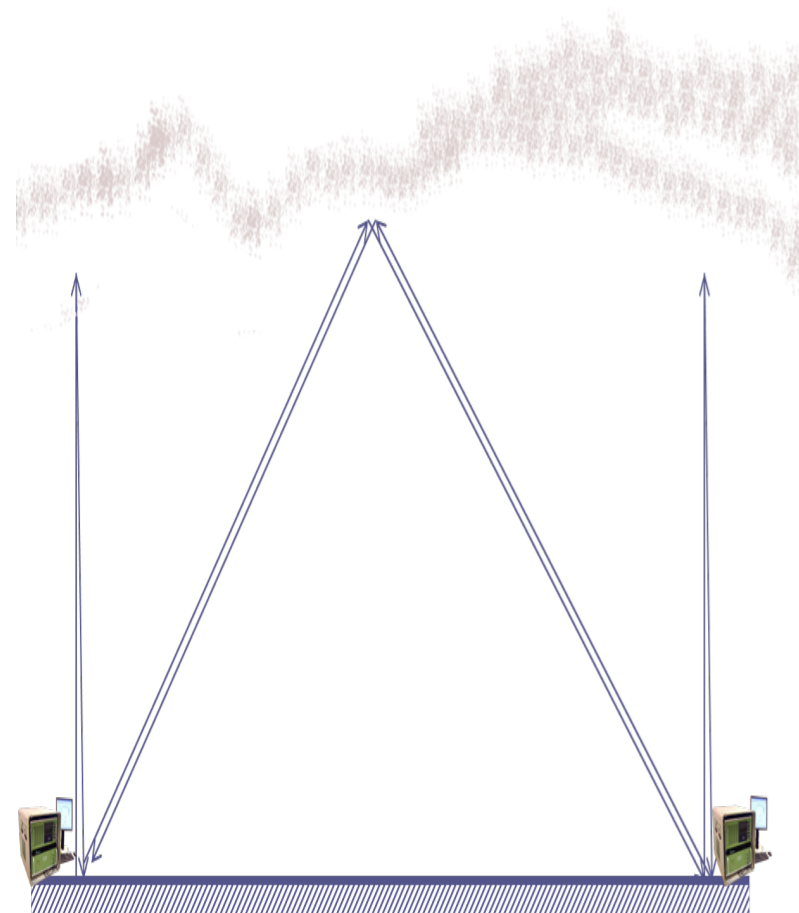


Belehaki A et al. 2020. An overview of methodologies for real-time detection, characterisation and tracking of traveling ionospheric disturbances developed in the TechTIDE project. J. Space Weather Space Clim. 10, 42.

<https://doi.org/10.1051/swsc/2020043>.

Altadill D et al. 2020. A method for real-time identification and tracking of traveling ionospheric disturbances using ionosonde data: First results. J Space Weather Space Clim 10, 2. <https://doi.org/10.1051/swsc/2019042>.

- **Ground Based sensors**

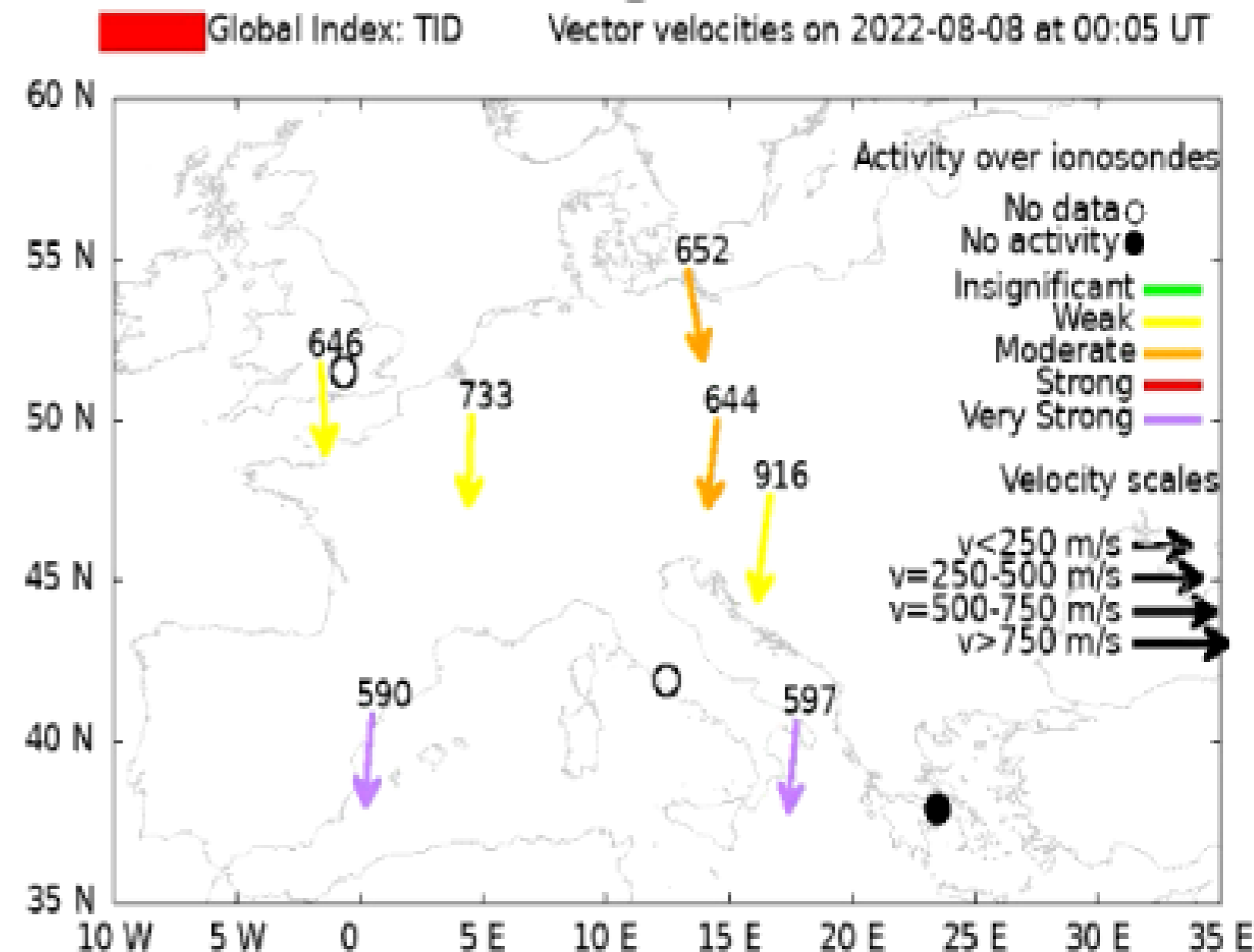
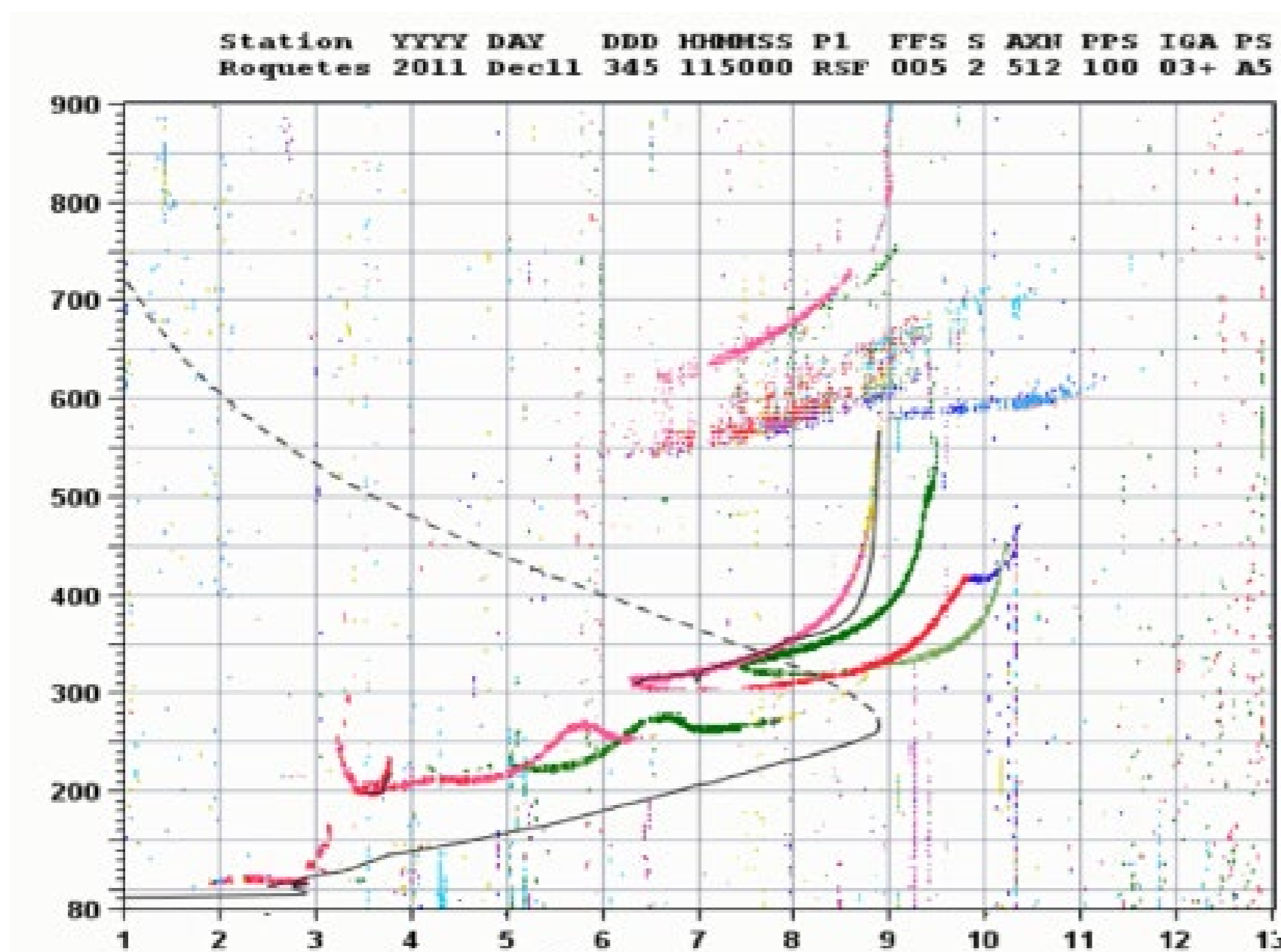


Belehaki A et al. 2020. An overview of methodologies for real-time detection, characterisation and tracking of traveling ionospheric disturbances developed in the TechTIDE project. *J. Space Weather Space Clim.* 10, 42.

<https://doi.org/10.1051/swsc/2020043>.

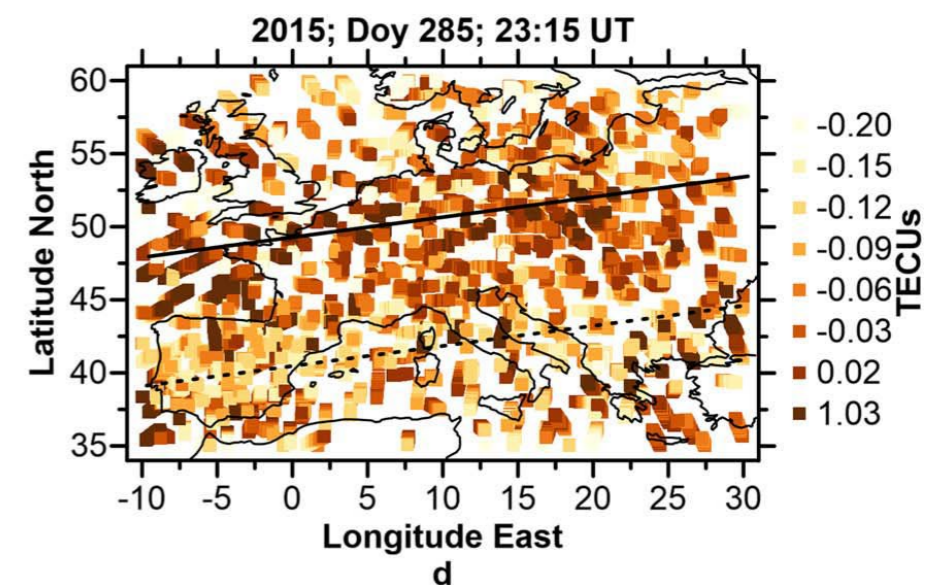
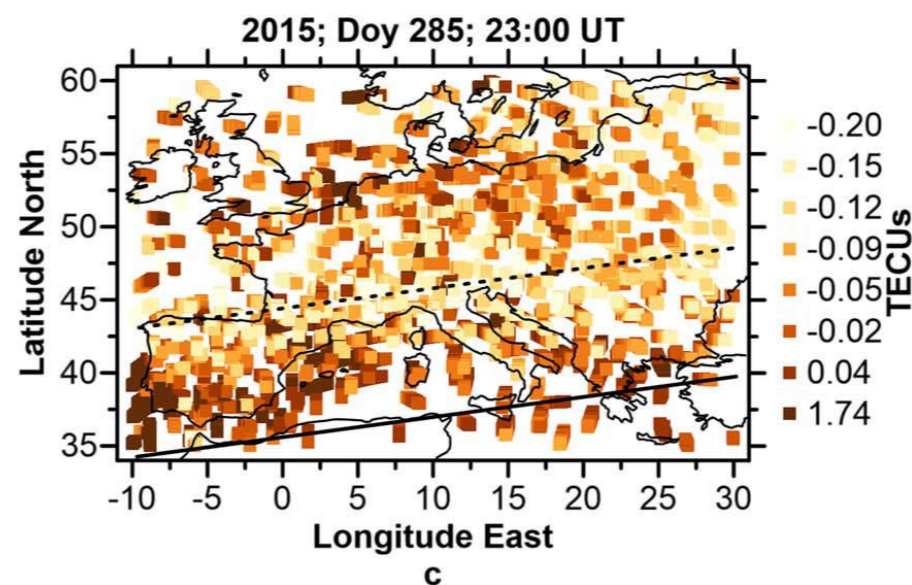
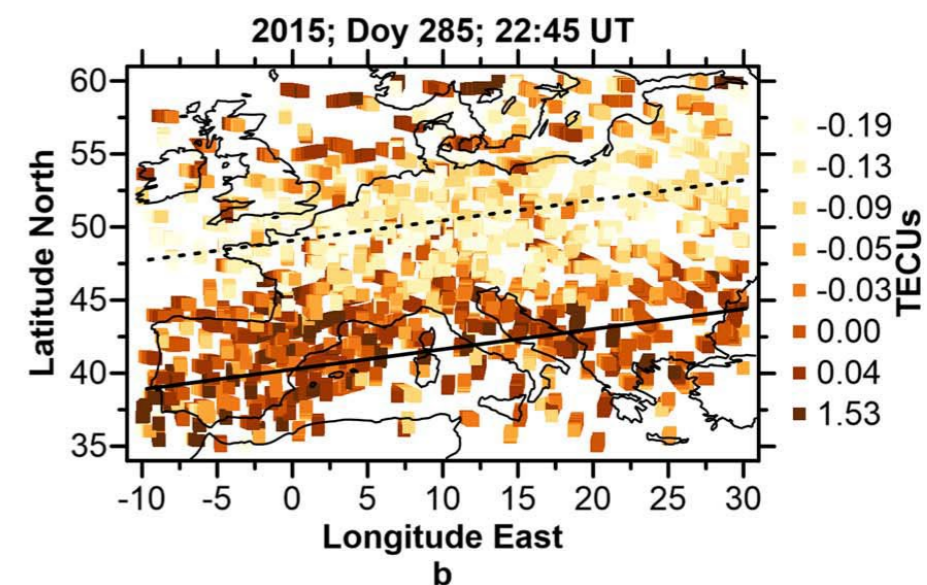
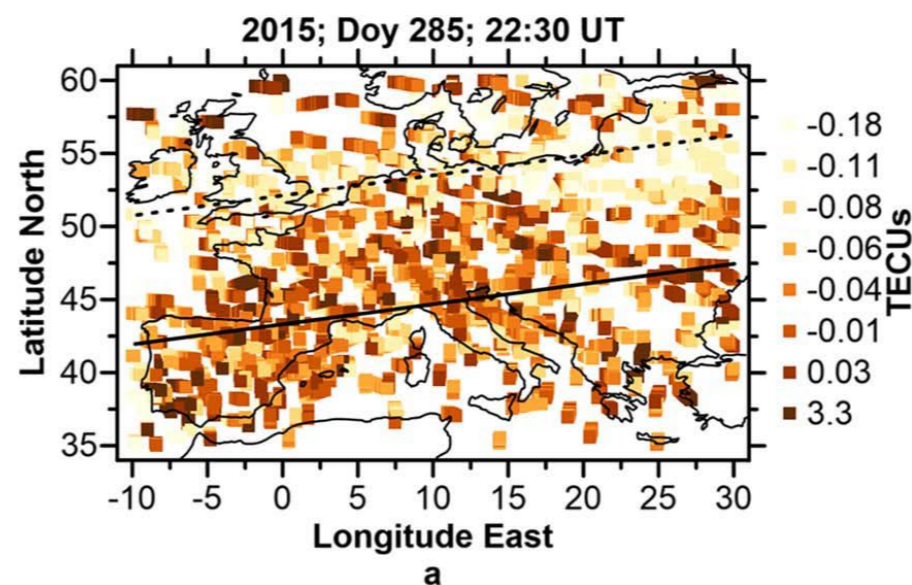
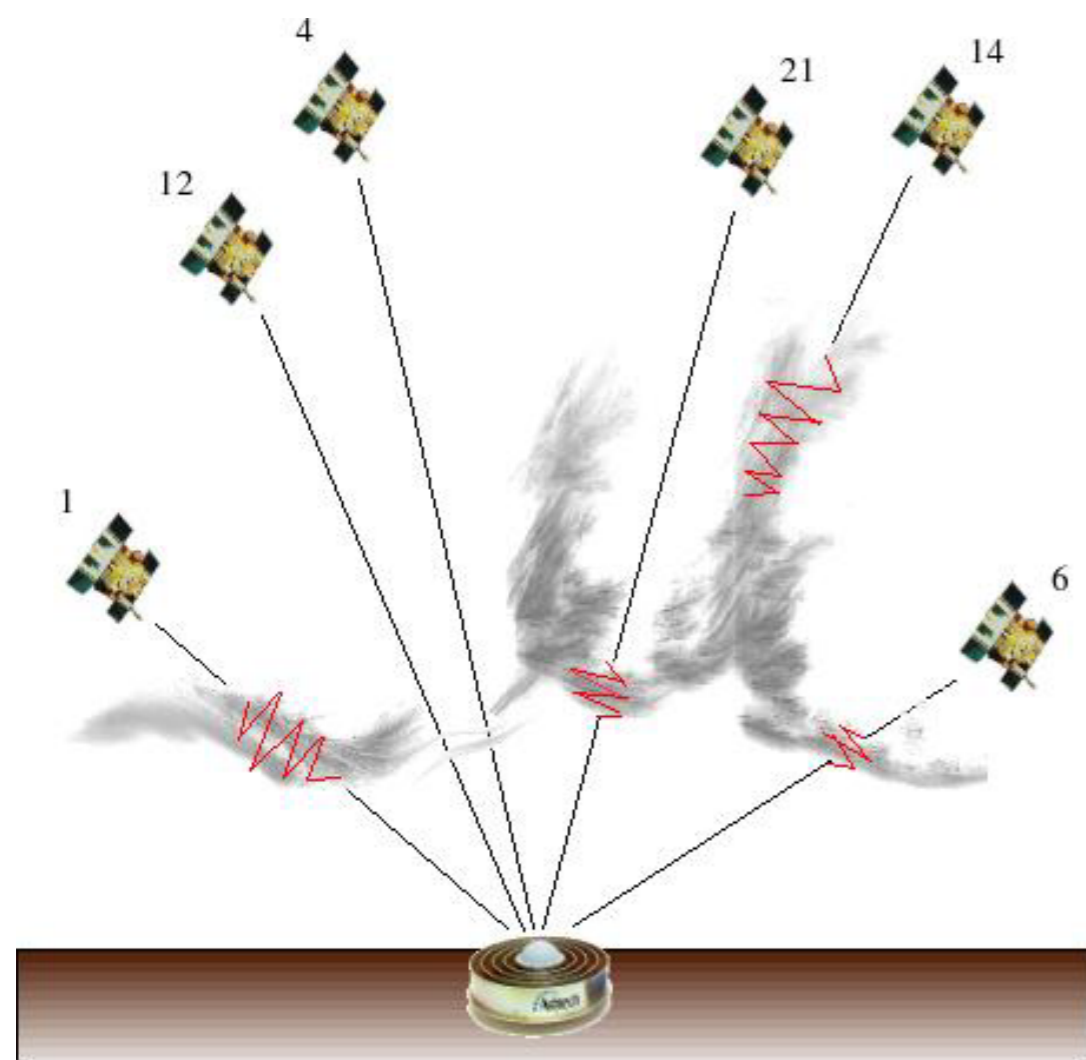
Altadill D et al. 2020. A method for real-time identification and tracking of traveling ionospheric disturbances using ionosonde data: First results. *J Space Weather Space Clim* 10, 2. <https://doi.org/10.1051/swsc/2019042>.

- **Ground Based sensors**



Altadill D et al. 2020. A method for real-time identification and tracking of traveling ionospheric disturbances using ionosonde data: First results. J Space Weather Space Clim 10, 2. <https://doi.org/10.1051/swsc/2019042>.

- **Satellite Based sensors**

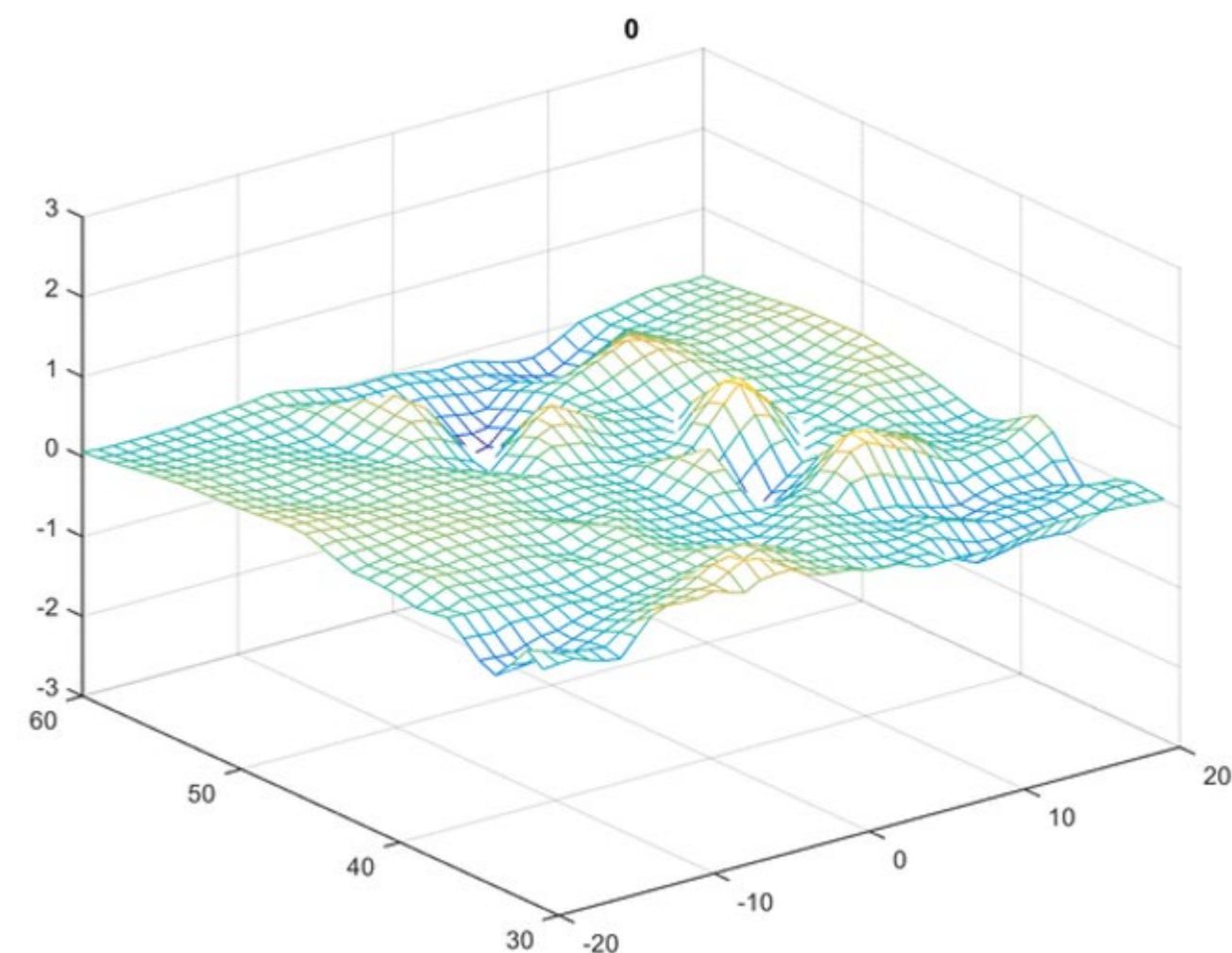
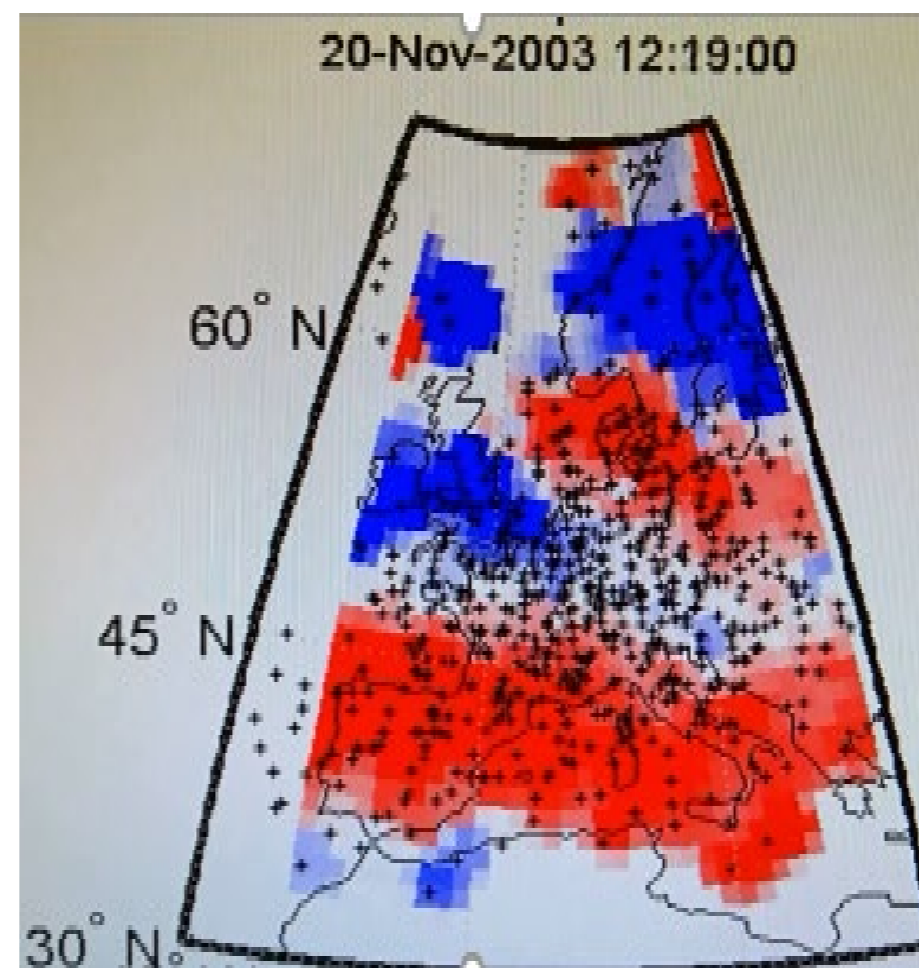
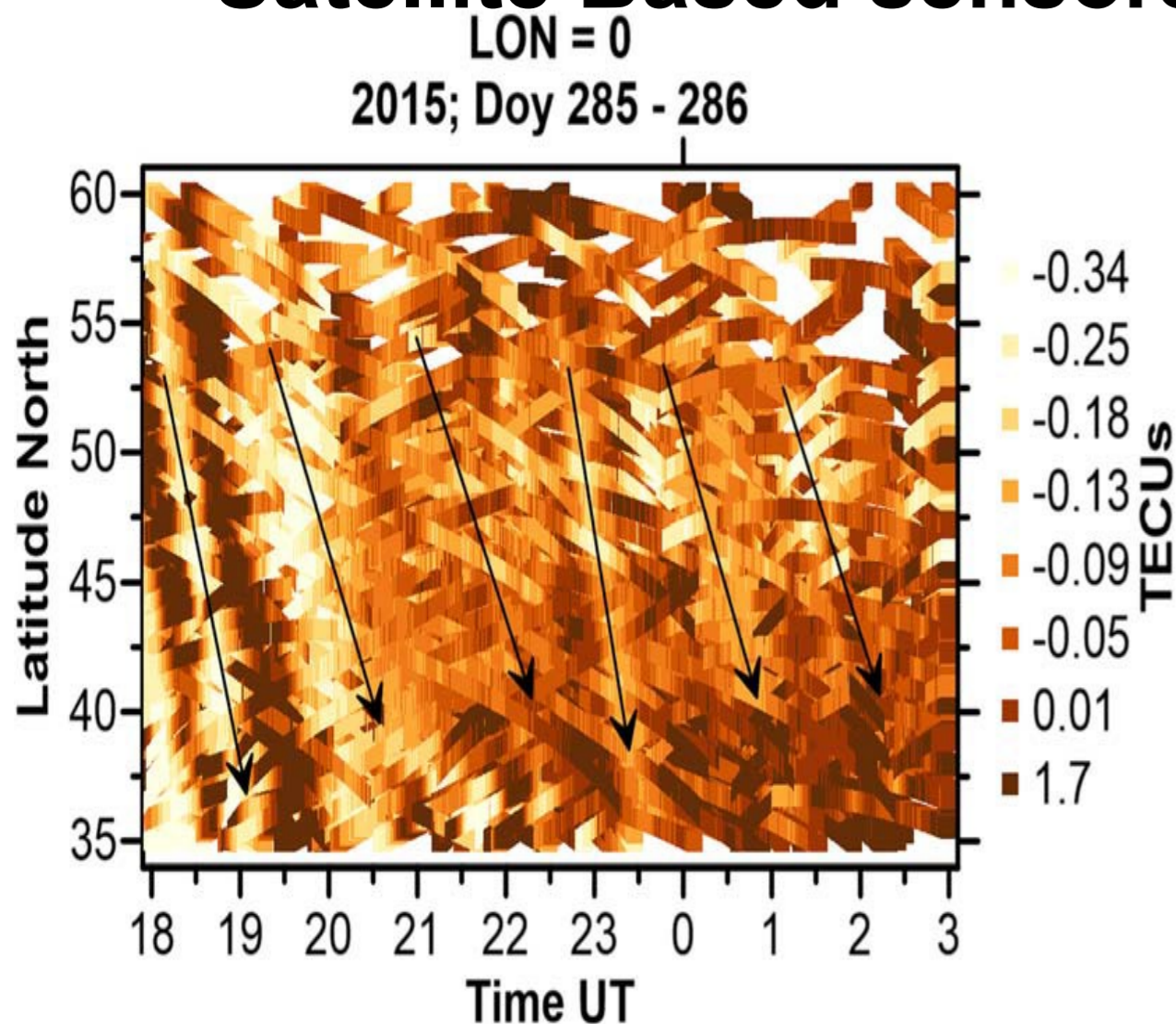


Belehaki A et al. 2020. An overview of methodologies for real-time detection, characterisation and tracking of traveling ionospheric disturbances developed in the TechTIDE project. *J. Space Weather Space Clim.* 10, 42.

<https://doi.org/10.1051/swsc/2020043>.

Altadill D et al. 2020. A method for real-time identification and tracking of traveling ionospheric disturbances using ionosonde data: First results. *J Space Weather Space Clim* 10, 2. <https://doi.org/10.1051/swsc/2019042>.

- **Satellite Based sensors**



Altadill D et al. 2020. A method for real-time identification and tracking of traveling ionospheric disturbances using ionosonde data: First results. J Space Weather Space Clim 10, 2. <https://doi.org/10.1051/swsc/2019042>.

Paznukhov V et al. 2020. Ionospheric tilt measurements: Application to traveling ionospheric disturbances climatology study. Radio Science, 55, e2019RS007012. <https://doi.org/10.1029/2019RS007012>.

Thank you for your attention!



**Funded by
the European Union**

The T-FORS project is funded by the European Union (GA-101081835). Views and opinions expressed are however those of the author(s) only and do not necessarily reflect those of the European Union or the European Health and Digital Executive Agency (HaDEA). Neither the European Union nor the granting authority can be held responsible for them.